MAGNETORESISTIVE PROPERTIES OF
$Sr_{4-x}La_xMn_3O_{10}$

A Dissertation Submitted to the Department of Physics, Bangladesh University of Engineering & Technology (BUET), Dhaka Bangladesh, In Partial Fulfillment for the Degree of Master of Philosophy (M.Phil)
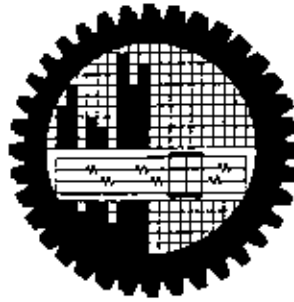
By

Shahanara Akter
Roll:100114013F

Department of Physics
Bangladesh University of Engineering & Technology (BUET)
Dhaka-1000, Bangladesh
March 2007

Candidate's Declaration

It is hereby declared that this thesis or any part of it has not been submitted elsewhere for the award of any degree or diploma.

Date: 31 March, 2007
BUET, DHAKA

Shahanara Akter
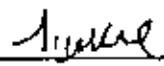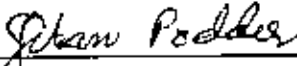Roll: 100114013F
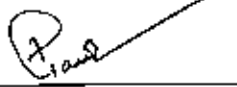Registration: 0110824
Session: October 2001

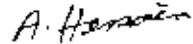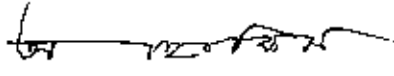## BANGLADESH UNIVERSITY OF ENGINEERING & TECHNOLOGY (BUET), DEPARTMENT OF PHYSICS, DHAKA-1000, BANGLADESH.

Certification of Thesis Work

The thesis titled "**Magnetoresistive properties of** $Sr_{4-x}La_xMn_3O_{10}$"submitted by **SHAHANARA AKTER** Roll No: 100114013F, Registration No: 0110824,Session: October-2001, has been accepted as satisfactory in partial fulfillment of the requirement for the degree of **Master of Philosophy (M.Phil)** in Physics on 31 March 2007.

BOARD OF EXAMINERS

1.   Chairman
Dr. Mominul Huq (Supervisor)
Professor, Department of Physics
BUET, Dhaka-1000,Bangladesh.

2.   Member
Dr. Jiban Podder (Ex. Officio)
Professor & Head, Department of Physics
BUET, Dhaka-1000, Bangladesh.

3.   Member
Dr. Md. Feroz Alam Khan
Professor, Department of Physics
BUET, Dhaka-1000, Bangladesh.

4.   Member
Dr. A.K.M. Akther Hossain
Associate Professor, Department of Physics
BUET, Dhaka-1000, Bangladesh.

5.   Member (External)
Dr. A.K.M. Abdul Hakim
Chief Engineer, Material Science Division
Atomic Energy Centre, Dhaka 1000

ABSTRACT

A series of polycrystalline bulk samples of $Sr_{4-x}La_xMn_3O_{10}$ were prepared using conventional solid state reaction technique and sintered at temperature $1100°C$ for 5 hours. The magnetoresistive properties of the polycrystalline bulk samples were investigated from room temperature down to liquid nitrogen temperature using standard four-probe technique. Analysis of X-ray diffraction pattern gives the single-phase structure of all the polycrystalline samples without any trace of impurity. The transition between ferromagnetic metallic and paramagnetic insulating states in $Sr_{4-x}La_xMn_3O_{10}$ perovskites is characterized by a maximum in the electrical resistivity at transition temperature. The transport behavior especially the metal-insulator (M-I) transition in manganites $Sr_{4-x}La_xMn_3O_{10}$ may be understood in terms of the double exchange mechanisms which involves the ferromagnetic coupling between $Mn^{3+}(t_{2g}^3 e_g^1)$ and $Mn^{4+}(t_{2g}^3 e_g^0)$ spins. As a result of strong Hund's exchange coupling, the itinerant e_g^1 electrons (holes) interact with the localized t_{2g}^3 electrons, and thus mediate ferromagnetic ordering and the simultaneous *M-I* transition. Substitution of La in place of Sr enhances % of Mn^{3+} which ultimately increases M-I transition temperature in these manganites. The M-I transition temperature is also found to increases due to the external magnetic field. The external field might suppress the spin fluctuations which improves the conductivity. The characteristic magnetoresistance was measured both at room temperature and liquid nitrogen temperature. At room temperature MR is very low and almost linear with field. At 78 K a sharp increase of MR was observed at low magnetic field but the MR gradually decreases with the increase of applied magnetic field. The activation energy curves show that the conduction occurred just above transition temperature through a thermally activated process.

Acknowledgement

This thesis is submitted in partial fulfillment of the requirements for obtaining the degree of M.Phil at the Bangladesh University of Engineering and Technology (BUET), Dhaka, Bangladesh. I would like to express my sincere gratitude to a number of people for their support, Collaboration and encouragement during the work has performed.

Firstly, I must thank my supervisor Professor Dr. Mominul Huq, Department of Physics, Bangladesh University of Engineering and Technology (BUET), Dhaka, who gave me an opportunity to carryout this research work under his scholastic supervision. I would like to express my deepest gratitude to my honorable supervisor for his guidance, constructive suggestions and constant inspiration in pursuing the investigation of the present research.

I would like to express my gratefulness to Professor Jiban Podder Head, Department of Physics, BUET, Dhaka, for his kind cooperation to do this research works. Also grateful to all faculty members of the department of Physics of BUET specially Dr. Md.Feroz Alam Khan. Dr.Md.Abu Hasan Bhuyan, Dr.Nazma Zaman, Dr. Nazrul Islam for their kind suggestion and valuable inspiration during this work.

I express sincere gratitude to Dr. A.K.M. Akther Hossain, Associate Professor, Department of Physics Bangladesh University of Engineering and Technology (BUET), Dhaka, for his kind co-operation and valuable suggestions throughout the work.

Thanks to Mr. Mohammed Abdul Basith, Lecturer Department of Physics Bangladesh University of Engineering and Technology BUET, Dhaka for his kind collaboration to carryout the experiment.

I would also express my sincere thanks to Head, Department of MME for permitting me use the laboratory facilities. I want to thanks Dr. Md. Fakhrul Islam, Department of MME for helping me to use high temperature furnace for sintering the samples. Thanks to Md. Yusuf Khan who helped me to perform the X-ray diffraction studies for characterization of the samples. Also thanks to other staff members of the mechanical workshop and welding shop of BUET for their collaboration.
I am also grateful to BUET authority for providing the financial grant for this research.

I remember with much gratefulness Prof. Md.Habibur Rahman Sarker, Principal, Sirajgonj Govt. College, Professor Gaziur Rahman, Ex. Principal, Sirajgonj Govt.College, Md. Asaduzzaman, Associate Prof Head, department of Physics, Sirajgonj Govt. College and all other colleagues in the physics department.

Sincere thanks to my friend Nazrul, Shampa, Hamid , Sumon, Taposhi for their friendliness support.

I am indebted to all my family members for their loving support and inspiration.

Date: SHAHANARA AKTER
March 2007   Department of Physics
                                                       BUET, Dhaka

Contents

LIST OF FIGURES

List of Tables

Notation
List of symbols

CMR	-Colossal magnetoresistance
GMR	-Giant magnetoresistance
MR	-Magnetoresistance
XRD	-X-ray diffraction
T_c	-Curie-Wiess transition temperature
Tp	-Phase transition temperature
T_N	-Neel temperature
°C	-Degree centigrade
K	-Kelvin
eV	-Electron volt
K_B	-Boltzman constant
J_H	-Hund's exchange interaction
AC	-Alternating current
DC	-Direct current
GB	-Grain boundary
JT	-Jahn-Teller distorn
e_g	-Two-fold degenerate state (doublet state)
t_{2g}	-Three-fold degenerate state
DE	-Double exchange
FM	-Ferromagnet
PM	-Paramagnetic metal
AF	-Antiferromagnetic metal
MR	-Magnetoresistance
MI	-Metal-Insulator transition
TCR	-Temperature coefficient of resistance
CFS	-Crystal Field Splitting
TMO	-Transition Metal Oxide
HTSC	-High temperature Superconductor
LFMR	-Low Field Magnetoresistance

CHAPTER 1

INTRODUCTION

1.1 INTRODUCTION

The mixed valance manganites have considerable research interest in recent years due to its interesting properties. In these manganites materials contains manganese in several valance states. This thesis presents results of an experimental study on magnetoresistive properties of a series of strontium-doped lanthanum manganese oxides. The magnetoresistance effect can be described a large decrease of the resistance on application of an external magnetic field and can be observed in some magnetic perovskites near the curie temperature. They are also called doped manganites and Perovskite manganites, because of their crystal structure resembles that of the mineral perovskite and sometimes doped manganites cause the substitution of RE (rare earth) cation with an M cation may serve as hole doping. The characteristic properties of the doped perovskite manganites are the CMR effect. CMR materials are interesting from a fundamental viewpoint. In contrast to traditional ferromagnets such as Fe, Co and Ni where the spin system is isolated from the lattice, in these manganites the charge, spin, and lattice degrees of freedom are strongly coupled together, leading to a delicate balance of interactions that gives rise to a rich variety of physical phenomena of current interest in condensed matter science. The discovery of colossal magnetoresistance (CMR) in mixed valance compounds with general formula $Ln_{1-x}A_xMnO_3$ (Ln = rare earth, A = alkaline earth) promoted a study of these type of compounds in the last years. Some of these perovskites exhibit fascinating properties like metal-insulator (M-I) transitions, charge ordering and ferromagnetism [1-4].

I

Perovskites are the n=∞ members of the more general family $(Ln,A)_{n+1}Mn_nO_{3n+1}$ called Ruddlesden-Popper type compound (RP).The CMR and M-I behavior found in perovskites are also exhibited by n=2 and 3 members of this family. These materials exhibit a resistance change when subjected to a magnetic field. The CMR effect is usually obtained at low temperature (below room temperature) and in high magnetic field, but the practical application demands the operating conditions both at room temperature and low magnetic field. The magnetic field sensitivity, the strong metal insulator transition at the curie temperature, the electric field polarizibility of the material and its subsequent effect on the transport properties, etc. are the properties of the rare earth manganites that could be exploited in a variety of devices.

The Ruddlesden-Popper (RP) type layered manganites, $T_{2-2x}D_{1+2x}Mn_2O_7$(where T is the trivalent rare earth cation like La, Nd, Pr etc. and D is the divalent alkaline earth cation like (Sr, Ca, Ba, etc.), have attracted considerable research interest due to its properties. The RP phases $A_{n+1}B_nO_{3n+1}$,consist of n layers of BO_6 corner-sharing octahedral blocks separated by rock salt AO layers. The observed colossal magnetoresistance (CMR) phenomena in these manganites are generally understood in terms of the double exchange mechanisms which involves the ferromagnetic coupling between $Mn^{3+}(t_{2g}^3 e_g^1)$ and $Mn^{4+}(t_{2g}^3 e_g^0)$ spins [5], However Millis et.al. [6] point out that the double exchange interaction doesn't explain the CMR alone [6].Other interactions such as charge-lattice and spin lattice interactions should be considered to elucidate the CMR[7].A small change in the chemical composition like the ratio between trivalent and divalent ions at the A site can induce a large change in the physical properties such as structural, magnetic, optical and electronic behaviour. A similar change can occur due to external effect such as magnetic field, a hydrostatic pressure or the temperature.

2

On partial doping of the trivalent RE–ion by divalent alkaline earth cation AE, leads to the formation of a mixed valance state of the Mn i.e. Mn^{3+} and Mn^{4+} to maintain the charge neutrality of the system. The perovskite ABO_3 type compounds with the three dimensional Mn-O-Mn such as $Sr_{4-x}La_xMn_3O_{10}$ is known to be conducting ferromagnets. The co-existence of metallic conductivity and ferromagnetic coupling in these materials has been explained in terms of double exchange mechanism [5-7]. The insulating $SrMnO_3$ material in which only Mn^{4+} exists, doping with the trivalent ions La causes the conversion of a proportion number of Mn^{3+} to Mn^{4+}. The transfer of an electron occurs simultaneously from Mn^{3+} to O^{2-} and from O^{2-} to Mn^{4+} is a real charge transfer process and involves overlap integral between Mn and O orbitals. Thus the observed CMR phenomena are understood in terms of the double exchange mechanisms which involves the ferromagnetic coupling between $Mn^{3+}(t_{2g}^3\ e_g^1)$ and $Mn^{4+}(t_{2g}^3\ e_g^0)$ spins [8-10]. Because of the strong Hund's coupling the doping enables e_g^1 electron of Mn^{3+} ion to hop to the neighboring Mn^{4+}, which mediates ferromagnetism and conduction. Millis *et.al.* point out that the double exchange interaction doesn't explain the CMR alone, because the curie temperature of most manganites, can't describe the huge magnitude of the CMR effect. Millis *et.al.*[6] argued that electron-phonon coupling due to Jahn -Teller distortion plays an important role to explain CMR effect. The above result suggests that there is considerable coupling among the charge, spin and lattice in this system. Several studies on the pseudocubic perovskites $La_{1-x}Sr_xMnO_3$ have shown that materials with carrier concentration x=0.3,which undergo a transition from the paramagnetic insulator state to the ferromagnetic metal state upon cooling, exhibit CMR in a narrow temperature range around the curie temperature.

In contrast to pseudocubic perovskite ($n=\infty$) with three-dimensional Mn-O networks, the layered versions of $(La-D)_{n+1}Mn_nO_{3n+1}$ consisting of perovskite blocks, $nMnO_6$

3

octahedra with an inverting layer of (La-M)O ions, possess a two dimensional anisotropic character whose magnitude depends on the n value. Apart from the n=1 member, which is an antiferromagnet at any doping concentration, the layered manganites with n=2 compound [11] have shown that they have remarkable features including MR ratio enhancement, magnetization, existence of two-dimensional ferromagnetic ordering at a certain temperature range, and the characteristic low temperature intrinsic MR effect. Very recently, it has been reported that the n=3 compound [12] exhibits some features that are similar to those observed for the n=2 compound. So far only a few papers have been published on n=3 members of the RP series. Brisi et $al.$[13] reported a tetragonal $Ca_4Mn_3O_{10}$ phase from an earlier x-ray powder diffraction analysis, which was considered to have lower symmetry in fact. Henry et $al.$ [14] studied $Ca_4Mn_3O_{10}$ and $Sr_4Mn_3O_{10}$ and reported that $Ca_4Mn_3O_{10}$ had a space group $Cec2$.Battle et $al.$[15] determined the structure of $Ca_4Mn_3O_{10}$ and reported a space group $Pbca$ according to X-ray and neutron diffractions. A dc magnetization study of $Ca_4Mn_3O_{10}$ was reported by Lago et $al.$[16] and attempts have been made to dope the n=3 member with La in order to induce mixed valence, though only small doping levels have been reported to date in bulk samples [17].

In the present investigation the divalent cation Sr^{2+} will be replaced by trivalent cation La^{3+} to study the electrical transport and magnetoresistive properties of triple layered perovskite manganites $Sr_{4-x}La_xMn_3O_{10}$.Hence present investigation aims to study the change in magnetoresistance, phase transition temperature and both the low temperature and high temperature transport mechanism of a series of bulk polycrystalline triple layered perovskite samples $Sr_{4-x}La_xMn_3O_{10}$ (x=0.5-2.5). This investigation is expected to help in understanding the CMR properties in n=3 members of the RP series and also to elucidate the consistency of the electrical transport and

magnetoresistive properties of these manganites with those of n=∞ and 2 members of the series [18.19].

Lago *et al.*[16] presented a detailed dc magnetization study of the compound $Ca_4Mn_3O_{10}$, which undergoes a transition into a G-type antiferromagnetic structure on cooling below 113.5 K. These materials behaves as a quasi-2D antiferromagnet in the temperature region below T_N. The resulting weak ferromagnetic component in each MnO_2 layer is hidden at zero field but an applied magnetic field induces a spin-flop transition to a phase with a net magnetization. A non-zero moment is observed at temperatures well above the antiferromagnetic transition and may responsible for the negative magnetoresistance.

Witte *et.al.* [17] studied the electrical and magnetic phases of the layered perovskite $Ca_{4-x}La_xMn_3O_{10}$ and found that the peak resistivity drops dramatically by five orders of magnitude in going from the undoped to the x=0.01 doped sample and a transition from paramagnetic insulator to a antiferromagnetic insulator i.e. a dramatic change in conduction mechanism. The large decrease in resistivity with doping and the appearance of uncompensated ordered magnetic moments suggests that upon further doping a FM phase should be expected.

Mihut *et.al.* [20] have investigated physical properties of the n=3 Ruddlesden-Popper compound $Ca_4Mn_3O_{10}$ and found that this compound adopts a layered structure in which a group of three perovskite layers alternate with single rock-salt layer. There is a sharp magnetic phase transition at 115K.The magnetoresistance is largest at low temperature. A 40% drop in resistivity is observed in a magnetic field of 14 T at 61K which exhibits colossal magnetoresistance.

1.2 Objective of the present studies

Our approach is to study the n=3 member of the (La, Sr) RP series with doping by La of the Sr i.e. electron doping so that the valence of Mn would decrease from 4.

To study the effect of substitution of La by Sr in electrical transport and magnetoresistive behavior of polycrystalline $Sr_{4-x}La_xMn_3O_{10}$.

To improve the value of transition temperature.

To understand the mechanism of CMR properties in these materials.

1.3 Sketch of the contents

In this work the preparation, characterization and magnetoresistive properties of the polycrystalline samples $Sr_{4-x}La_xMn_3O_{10}$ (x=0.5,1.0,2.0,2.5) were described.

Chapter 2 gives a brief description of the existing theories and mechanism of CMR manganites. Various points for understanding the electronic structure of manganites including the atomic view, double-exchange theory, Jahn-Teller effects and various range of hopping in manganites are discussed briefly.

Chapter 3 describes the methods of sample preparation and characterization techniques for synthesis of manganese oxide materials.

Chapter 4 presents result on magnetoresistive properties of polycrystalline samples $Sr_{4-x}La_xMn_3O_{10}$ for various doping level.

Chapter 5 summarizes the findings of this research.

References

[1]   Rao C.N.R., Arulraj A.,Cheetham A.K., Raveau B.,(2000),*"Charge ordering in the rare earth manganates:the experimental situation"*, J. Phys: Condens. Matter **12**, R83- R106.

[2]   Von Helmot R.,Wecker J., Holzapfel B., Schultz L., Samwer K., (1993). *"Giant negative Magnetoresistance in perovskite like $La_{2.3}Ba_{1.3}MnO_3$ ferromagnetic films"*, Phys. Rev. Lett. **71**, 2331-2333.

[3]   Martin C., Maignan A., Damay F., Hervieu M., Raveau B., Hejtmanek J., (2001),*" J. Solid State Chem. Electron doping in $CaMnO_3$ induced by Mo for Mn substitution: An efficient route to orbital and charge ordering"*, Phys. Rev. B **63**, 100406-100410.

[4]   Rao C. N. R., Anthony Arulraj., Santosh P. N. and Cheetham A. K., (1998), *"Charge Ordering in Manganates"*, Chem. Mate. **10** (10), 2714 –2722.

[5]   Zener C., (1951),*"Interaction between the d-shells in the Transition metals.(II.) ferromagnetic Compounds of Manganese with Perovskite structure"*, phys. Rev. **82**, 403-405.

[6]   Millis A.J., Littlewood P.B., Shraiman B.I., (1995),*"Double exchange alone can not explain the Resisviry of $La_{1-x}Sr_xMnO_3$"*, Phys. Rev. Lett .**74**, 5144-5147.

[7]   De Teresa J.M., Ibara M.R., Algarabel P.A., Ritter C., Marquina C., Garcia J., Del Moral A., Arnold Z.,(1997),*"Evidence for magnetic polarons in the magnetoresistive perovskites"*, Nature **386**, 256-259.

[8]   Goodenough J.B., (1955), *"Theory of the role of Covalence in the Perovskite-type Manganites [La,M(II)]MnO3"*, Phys. Rev. **100**, 564-573.

[9]   Anderson P.W., Hasegawa H., (1955), *"Considerations on Double Exchange"*, Phys. Rev. **100**. 675 -681.

[10]   Moritomo Y., Tomioka Y., Asamitsu A., Tokura Y.,(1996), *"Giant magnetoresistance of manganese oxides with a layered perovskite structure"*, Nature (London) **380**.141.

[11]   Asano H., Hayakawa J.and Matsui M.,(1996),*"Two-dimensional ferromagnetic ordering and magnetoresistance in the layered perovskite $La_{2.2x}Ca_{1.2x}Mn_3O_7$"*, Appl. Phys. lett. **68**, 3638-3640.

[12]   Asano H., Hayakawa J. and Matsui M.,(1997),*"Magnetotransport in perovskite series $La_{n-nx}Ca_{1+nx}$ Mn_nO_{3n+1} ferromagnets"*, Appl. Phys. Lett. **71**, 844.

[13]   Brisi C. and Lucco-Borlera M., Inorg J.,(1995),*"Studies of the $Ca_4Mn_3O_{10}$ structure obtained using high pressure and high temperature"*, Nucl. Chem. **27**, 2129.

[14]   Henry J.R., Peter G., Shaun B., Robert H. M., Shane J. K., Tim J. W., Frank J. L. and Keith S. M., (1996),*"Ideal $n = 3$ phase $Ca_4Mn_3O_{10}$ of Ruddlesden–Popper series obtained using high pressure and high temperature"*, Aust. J. Chem. **49**, 205.

[15]   Battle P.D., Green M.A., Lago J., Millburn J.E., Rosseinsky M.J. and Vente J.F., (1998), *"Crystal and magnetic Structure of $Ca_4Mn_3O_{10}$, an $n=3$ Ruddlesden-popper Compound"*, Chem. Mater **10**,658.

[16]   Lago J., Battle P. D. and Rosseinsky M. J.,(2000), *"Weak ferromagnetism and spin-glass behaviour of the $n = 3$ Ruddlesden-Popper compound $Ca_4Mn_3O_{10}$: a dc magnetization study"*, J. Phys.: Condens. Matter **12**, 2505-2524.

[17]   Witte N.S., Goodman P.,Lincoln F.J., March R.H. and Kennedy S.J.,(1998),*"Electrical and magnetic phase of the layered perovskite $Ca_{4-x}La_xMn_3O_{10}$"*, Appl. Phys. Lett. **72**, 853.

[18]   Rodrguez-martinez Lide M. and Attfield Paul J., (1996),*"Cation disorder and size effects in magnetoresistive manganese oxide perovskites"*, Phys. Rev. B **54**, R 15622 -15625.

[19]   Shen C.H., Liu R.S., Lin J.G, Huang C.Y. and Sheu S.H., (1999), *"Structural, electrical and magnetic properties of two-dimensional $La_{1.2}(Sr_{1.8}-xCa_x)Mn_2O_7$ manganites"*, J. Appl. Phys. **86**, 2178.

[20]   Mihut A.I., Battle P.D., Lago J., Millburn J.E., Rosseinsky M.J. and Vente J.F., (1998), *"Physical properties of the $n = 3$ Ruddlesden-Popper Compound $Ca_4Mn_3O_{10}$"*, J. Phys: Condens. Matter. **10**, L 727-L 735.

CHAPTER 2

LITERATURE REVIEW AND PHYSICAL PROPERTIES OF MIXED VALENCE MANGANITES

2.1 Introduction

The historical overview of manganite materials, various issues of colossal magnetoresistance (CMR) in manganites, which is very important, is discussed in this chapter. Theoretical explanation of CMR materials including the electronic structure of the manganites is described briefly. The bulk magnetic and transport properties of manganites and various phase diagrams as a function of doping, temperature, external magnetic field and hydrostatic pressure etc. are also presented here, various models of low temperature magnetoresistance and grain boundary magnetoresistance in the doped manganites are also discussed.

2.2 Historical Overview of manganites

Due to the magnetic transition on the electronic conduction manganites materials are very important for the present technology. The discovery of colossal Magnetoresistance (CMR) in doped perovskite manganites revolutionized material science and a lot of effort has been carried out (and still going on) to find out materials with improved magnetoresistance around room temperature at low magnetic fields. The analogies with manganites and other magnetoresistive materials are based on the presence of large magnetoresistance, a competition between FM and AF states and universally accepted in homogeneities. Based on above analogies, the magnetoresistive family consists of large number of materials having different crystalline structures. These mixed valance manganites have been studied for more than five decades but are still considered modern materials because of their wide

potential for technological applications. The brief history of various research work of perovskite manganites are given bellow:

About half a decade ago Jonker and Santen (1950) [1-3] described the preparation of polycrystalline samples of $(La,Ca)MnO_3, (La,Sr)MnO_3$ and $(La,Ba)MnO_3$ manganites and reported ferromagnetism and anomalies in the conductivity at the curie temperature with variation in lattice parameter as a function of hole doping. Few years later Volger observed a notable decrease of resistivity for $La_{0.8}Sr_{0.2}MnO_3$ in FM states in applied magnetic field [4].

In 1970, Searle and Wang [5-6] also reported the same behaviour based on single crystals. A year later, Jin $et.al.$ [7] reported that it is possible to reduce the resistivity by several orders of magnitude under the application of very large magnetic field in hole doped manganese oxide perovskites near the curie temperature T_c.

A burst of research activity on manganites started during 1990 because of the observation of large magnetoresistance Kusters $et.al.$ (1989) [8] on bulk $Nd_{0.5}Pb_{0.5}MnO_3$ reveals the large MR effect. Another work by von Helmholtz $et.$ $al.$ (1993) [9] on thin films of $La_{2/3}Ba_{1/3}MnO_3$ also revealed a large MR effect at room temperature thereafter similar conclusion was reached by Chahara et $al.$(1993)[10] using thin films of $La_{3/4}Ca_{1/4}MnO_3$ and Ju $et.$ $al.$ (1994)[11] for films of $La_{1-x}Sr_xMnO_3$.They all observed MR values larger than those observed in artificially engineered multilayers (GMR) [12].

In a study Sun $et.$ $al.$ (1997)[13] examined a series of compounds at constant 33% dopant level $La_{3/2-x}R_xCa_{1/3}MnO_3$(R=Pr, Nd, S, Eu, Gd, Tb, Y, Er, Tm) with x chosen to fix at tolerance factor $t=0$ under the constrains of constant doping level x and t, Hwang et $al.$ (1999) [14] would predict no variation of insulator-metal transition

10

temperature (T_{DM}) with rare earth. Sun *et al.* (1997) did observe a dependence of T_{DM}, which demonstrates that a single, tolerance factor 't' is inadequate for describing the behavior of perovskite manganites, where A-site component have widely different radii. They attributed discrepancy due to an inhomogeneous distribution of cat ions on the A-site [13].

Millis *et al.* (1995) [15] incorporated the idea that double exchange alone does not explain the resistivity of $La_{1-x}Sr_xMnO_3$.Roder *et.al.* (1996) [16,17] incorporated Jahn-Teller (electron-phonon) coupling in to the double exchange model and suggested that the e_g charge carrier becomes self trapped as localized lattice distortions with a spin polarization around the position of charge carrier, having a coherence length of the order of five Mn sites. Vibronic model of Goodenough (1997) [18]. Bi-polaronic model of Alexandrov (1999) [19], magnetoimpurity theory of Nagev (2001) [20] and Falicov-Kimball like approach of RamaKrishnan T.V., (2004) [21] etc. explains some aspect or the other of doped perovskite manganites, but a satisfactory theory of manganites is still lacking.

Wollan and Koehler (1995) [22] draw the first magnetic structures of $La_{1-x}Ca_xMnO_3$ by neutron diffraction. In their studies they explain charge-ordering and mixed phase tendencies in the manganites.

2.3 Colossal magnetoresistance

Manganese oxides with a perovskite structure[23] exhibit a transition between a paramagnetic insulating phase and a ferromagnetic metal phase. Associated with this transition there is an effect known as colossal magnetoresistance[24,25] (CMR)—in the vicinity of the transition temperature, the materials exhibit a large change in resistance in response to an applied magnetic field. Such an effect, if optimized, might

find potential application in magnetic devices. But the criteria for achieving (and hence optimizing) CMR are not clear, presenting a challenge for materials scientists.

In 1993, materials were found that could change their resistance not by a few percent but by orders of magnitude. The obtained magnitude of MR in these materials was very large; close to 100%, for this reason, many researchers prefer to call this colossal magnetoresistance, as distinct from GMR. Magnetoresistance (MR), the ability of a material to vary its electrical resistance depending on an applied magnetic field. In the other way, Magnetoresistance (MR) refers to the relative change in the electrical resistivity of a material on the application of an external magnetic field. For that reason, over recent years magnetoresistance has been the center of many investigations primarily due to applications in magnetic storage and sensing device. The resistivity of some materials is greatly affected when the materials is subjected to a magnetic field. This phenomenon is known as magnetoresistance. One of the most important properties of the manganites is the influence of a magnetic transition on the electronic conduction. It has been observed that doped manganese oxide ceramics exhibits a very large magnetoresistance [26-29], about 99% for some samples in the presence of 10T applied magnetic field. This phenomenon is called colossal magnetoresistance.

$$MR\% = - \frac{\rho(H) - \rho(0)}{\rho(0)} \times 100$$

Where $\rho(H)$ and $\rho(0)$ are the resistivities at a given temperature in the applied and zero magnetic ferromagnetic metals such as Fe and Co. Cu is more typical in that the same very powerful field (24T) gave rise to change of only ~2% at room temperature. This MR originates from the impact of the Lorentz force on the moving charge carries similar to the Hall effect. Its values is ~10% at 10T. A classification of magnetoresistance phenomenon is based on the distinction familiar in magnetism

12

between intrinsic properties such as anisotropy constants, which depends only on the crystal structure, composition and purity, and extrinsic properties such as coercivity which depend on the structure on a mesoscopic or microscopic length scale.

One of the most interesting properties of the manganites is the influence of a magnetic transition on the electronic conduction. In 1950, Jonker and Van Santeen discovered that the resistance below the magnetic ordering, the curie temperature T_c , exhibits a positive thermal co-efficient, indicating metallic-like behavior and a negative gradient above T_c [1-3] based on measurements of polycrystalline ceramics. In 1970, Searle and Wang [5-6] also reported the same behavior based on single crystals .A year later, Jin et.al. [30] reported that it is possible to reduce the resistivity by several orders of magnitude under the application of very large magnetic field in hole doped manganese oxide perovskites near the curie temperature T_c. Giant magnetoresistance is caused by introducing interfaces in spin polarized conductors and is restricted below T_c, where as CMR, is a bulk property which originates from magnetic ordering and is usually confined to the vicinity of T_c. In particular, Jin et al. [7,] reported, maximum values of around 100,000% for thin films of calcium doped manganese oxide near 77K with applied magnetic fields of 6T. They also remarked that their results had a very strong dependence on the method used to grow the films. Interest in the potential applications of colossal magnetoresistance was soon prompted by the complexity of the materials. In these materials, the interaction between the electrons and lattice vibrations is unusually strong, leading to a wide range of striking physical phenomena and most crucially, can be "tuned" over a wide range by variation of chemical composition, temperature and magnetic field [31]. These materials provides an opportunity to study the poorly understood physics of systems in which a high density of electrons is strongly coupled to phonons that demand a microscopic, and ultimately atomic, characterization of structure, electronic structure and dynamics. The relationships

13

between these structural, electronic, magnetic and optical properties are to be explained in a systematic way.

2.4 Crystal Structure and its Relevance

The characteristic properties of doped perovskite manganites like the CMR effect and the strong correlation between the structure and electronic magnetic phases can all be attributed to the ratio of the Mn^{3+} and Mn^{4+} ions. The parent compound crystallizes in $AMnO_3$ type having general $RE_{1-x}AE_xMnO_3$, where RE stands for trivalent rare earth cat ion .Such as La, Pr, Nd, Sm, Eu, Gd, Tb, Y etc. and AE Stands for divalent alkaline earth cat ion such as Ca, Br, Sr etc. In this perovskite like structure (RE, AE) occupies the vertices of the cubic unit cell, Mn occupies the body center and O occupies the six faces of the cube, which forms MnO_6 octahedra. On partial doping of the trivalent RE-ion by divalent alkaline earth cat ion AE, leads to the formation of a mixed valence state of the Mn i.e. Mn^{3+} and Mn^{4+} to maintain the charge neutrality of the system (e.g. $La_{1-x}^{3+} Ca_x^{2+} Mn_{1-x}^{3+} Mn_x^{4+} La_{1-x}^{3+}$). The mixed valency of the Mn ions may also be controlled by varying the oxygen content [32-33]. This doping with some divalent cat ion causes the structure to get distorted due to the differences in the size of the various atoms and leads to Jahn-Teller effect.

(a)   (b)   (c)
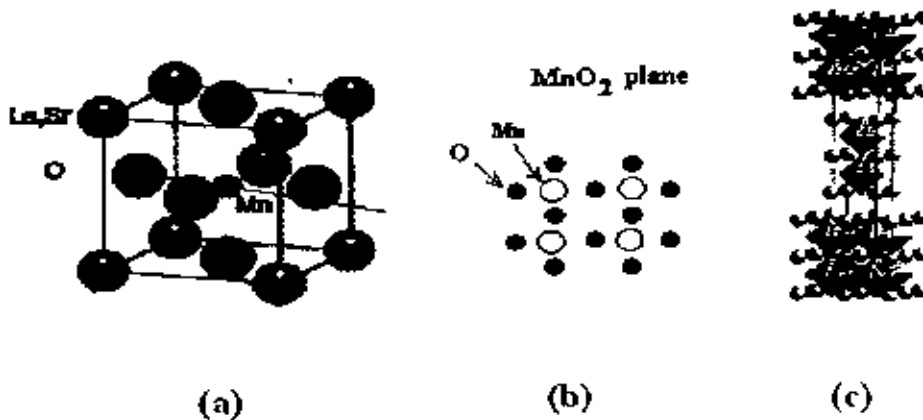
Figure 2.1: Crystal structures of the most important oxides: (a) perovskite structure ($La_{0.7}Sr_{0.3}MnO_3$); (b) The MnO_2 plane, which is identical in the structure to the CuO_2 planes of the high temperature superconductors (HTSC's). (c) n = 2 Ruddlesden–Popper phase ($La_{1.2}Sr_{1.8}Mn_2O_7$, MnO_6 octahedra are shaded, La/Sr ions are drawn as sphere).

As modifications from the cubic structure due to doping, perovskite-based structures show lattice distortion. One of the possible origin in the lattice distortion is the deformation of the MnO_6 octahedron arising from the Jahn-Teller effect that is inherent to high-spin(s=2) Mn^{3+} with double degeneracy of e_g orbitals. Another lattice deformation comes from the connection pattern of the MnO_6 octahedra in the perovskite structure, forming rhombohedral or orthorhombic lattice. Such a distortion of perovskite $AMnO_3$ (where $A=RE_{1-x}AE_x$) governed by the Goldsmith tolerance factor 't' [34,35] which measures the deviation from perfect cubic symmetry (t =1) and is defined by,

$$t = \frac{d_{A-0}}{\sqrt{2d_{Mn-0}}} = \frac{\langle r_A \rangle + r_0}{\sqrt{2}(\langle r_A \rangle + r_0)}$$.

Where, d_{A-0} is the distance between the A-site, where the lanthanide or alkaline earth ions are located, to the nearest oxygen ion i.e. ($<r_A>+r_0$) and d_{Mn-0} is the Mn–O shortest distance which are calculated from the sum of the ionic radii for 12-co-ordinated cat ions and 6-co-ordinated Mn-cat ions. However, the tolerance factor is depending on both temperature and pressure. Since for an undistorted cube the Mn–O–Mn bond is straight ($d_{A-0}= \sqrt{2}d_{Mn-0}$) that makes t =1. However sometimes the A - ions are too small to fill the space in the cubic centers and due to that the oxygen tend to move toward the center, reducing d_{A-0} (d_{Mn-0} also changes at the same time). For this reason, the tolerance factor becomes smaller than one, t<1, as the A-site radius is reduced. and the Mn –O– Mn angle gets smaller than 180°. The hopping amplitude for carriers to move from Mn to Mn naturally decreases as O is reduced from 180° [37]. Thus as the tolerance factor decreases the tendencies of charge localization increases due to the reduction in the carrier mobility. For the ideal cubic structure t =1, but the stable perovskite structure occurs over a range of 0.8<t<1.1.For lower values of 't', the cubic structure is distorted to optimize the A-O bond lengths. This

distortion affects the conduction band which appears as hybridization of the P-level of oxygen and the e_g levels of the Mn. The orbitals overlap decreases with decrease in tolerance factor. Sun *et.al.* (1997) did observe a dependence of insulator metal transition temperature T_{IM} on the choice of rare earth ion, which demonstrates that a single, average tolerance factor 't' is inadequate for describing the behavior of perovskites manganites where, A-site components have widely different radii. They attributed discrepancy due to an inhomogeneous distribution of cat ions on the A-Site [36].

2.5 Electronic structure of the manganites

2.5.1 Physical Overview of doped manganites

The important manganite, $La_{1-x}Sr_xMnO_3$ (LSMO) is widely studied as a representative of large band width Mn-oxides and has a high curie temperature of 370K at intermediate hole doping [38]. In the LSMO compound a structural transition from orthorhombic (x>20%) to rhombohedral (x<20%) is present [39]. However, the structural phase diagram is even richer. In general the orthorhombic phase is stable at lower temperatures while the rhombohedral phase requires higher temperature. Thus depending on doping, one can thus obtain ferromagnetic or antiferromagnetic metallic phases as well as antiferromagnetic insulating phase. Ferromagnetic insulators are less common, since the occurrence of ferromagnetism is associated with the movement of free carriers in the lattice, but can be obtained for some partial orbital ordering cases. Mixed valence manganites, with the composition $AMn^{3+}O_3$ or $BMn^{4+}O_3$ is one family of the larger group of transition metal oxides, which includes other families such as Ferro electronic titanites. Some manganites can be formed of hexagonal layered crystal structures which are different from the cubic structure in atomic view, play some important role resulting different physical characteristics [40]. The CMR

materials of the form (RE) $_{1-x}$A$_x$MnO$_3$ have attracted most of the research efforts. RE stands for a rare earth ion such as La, Nd, Pr or Gd and A denotes a divalent ion such as Ca, Sr or Ba. The Manganites crystallize in the perovskite structure, figure-2.2. The Ruddlesden-popper family of compounds (RE,A)$_{n+1}$Mn$_n$O$_{3n+1}$ crystallize in a orthorhombic structure consisting of n=3 member of vertex sharing MnO$_6$ octahedra extending in the ab-plane and having a thickness of an octahedra along the c-axis shown in the following figure .

(a)   (b)
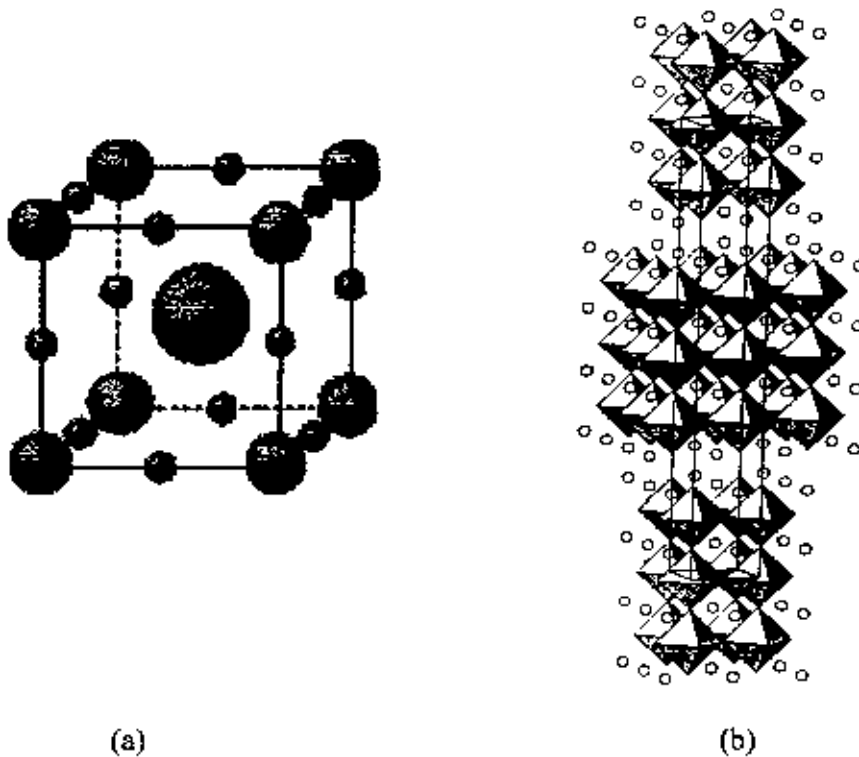
Figure: 2.2 (a) Crystallographic Structure of general ABO$_3$ type Cubic Perovskite, (b) Crystallographic Structure of n=3 layered orthorhombic perovskite.

The Perovskite crystal structure can be regarded as a three dimensional network of corner sharing MnO$_6$ octahedra, with Mn ions in the middle of the octahedral. Eight octahedra form a cube. with the A-site in its center. In the cubic perovskite, the A-site is twelve fold surrounded by oxygen ions. But typically the ionic radius of the A ion is

17

similar than the volume enclosed by the oxygen ions. This volume reduced by rotating the octahedra with respect to each other. In the undoped parent compound $Sr_4Mn_3O_{10}$, the crystal structure containing triple groups of face-shared MnO_6 octahedra interconnected by common corners into a two-dimensional framework. In figure 2.2(b) the n=3 RP structure, shows the three layers of MO_6 octahedra along the c-axis separated by an insulating rock-salt layer.

The spins are ordered ferromagnetically in the ac plane with the spins parallel to a-axis [41]. There is a antiferromagnetic coupling between the layers: along the b-axis which is close to 180° [42]. In manganites family the widely known chemical formula $R_{1-x}A_xMnO_3$ (where R is a rare earth such as La, Nd, Pr and A is divalent alkali such as Sr, Ca, Ba, Pb). In general R and A are also be compound of two different cations, for instance $(La_{1-y}Pr_y)_{1-x}CaMnO_3$. The Oxygen has full outer shell (2p) being in an O^{2-} state. Mn presents two oxidation states Mn^{4+} and Mn^{3+}, namely this is a mixed valency compound, $R_{1-x}^{3+}A_x^{2+}Mn_{1-x}^{3+}Mn_x^{4+}O_3^{2-}$. In order to get charge neutrality, the ratio Mn^{3+}/Mn^{4+} is equal to the ratio R^{3+}/A^{2+}. The extreme compounds x=0 and x=1 are not mixed valent, Therefore, doping with atom A is equivalent to change the valence of the Mn ions from 3+ to 4+, Which creates a mixed valence of manganites.

2.5.2 Ionic view of Electronic structure

Figure 2.3 shows the electronic configuration for the Mn^{3-} and Mn^{4+} ions in the compound $AMnO_3$ in a hybrid orbital structure. Mn ions have an incomplete d-shell $(Mn:[Ar]3d^54s^2)$. According to Hund's rule, in order to minimize the energy, all the unpaired electrons in the outer d-shell have their spins parallel to one another, thus, only the five d-levels corresponding to the majority spin are accessible.

The five d levels are split in e_g (two degenerate levels, $d_{x^2-y^2}$ and $d_{3z^2-r^2}$) and t_{2g} (three degenerate levels, d_{xy}, d_{yz} and d_{zx}) due to the cubic crystal field. This splitting has been estimated to be around 1 eV. [23]. Jhan-Teller (JT) distortions act on Mn^{3+} leading to a further splitting. The two e_g levels are then separated in energy around 0.25eV. The t_{2g} levels are also split due to JT distortions, but this has not any relevance for the system as the electrons living there are completely localized. Only the majority spins levels are shown. The minority spins levels are much higher in energy (due to Hund's coupling which can be several eV).
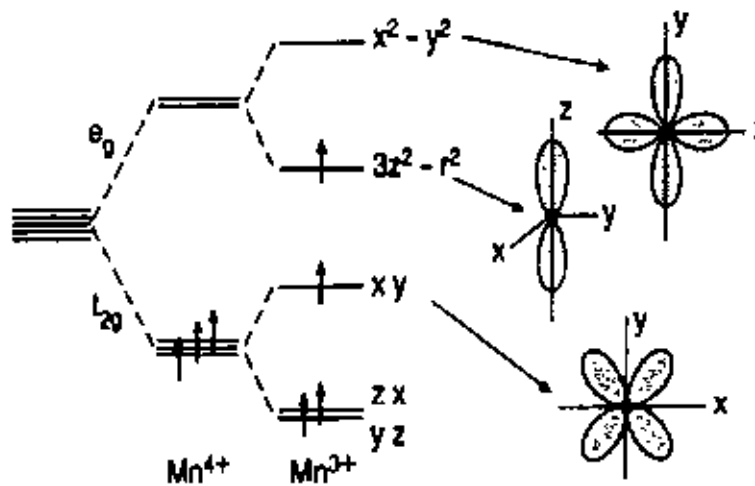
Figure: 2.3 Electron state of the outermost 3d energy level of the Mn^{3+} and Mn^{4+} ions. The five d levels are split in e_g (two degenerate levels, $d_{x^2-y^2}$ and $d_{3z^2-r^2}$).

Hund's rule is implied by two interactions: coulomb repulsion makes electrons to be in a different d-orbital each; Hund's coupling obliges the electrons spins to be parallel. In isolated atoms, the five d-orbitals are degenerate but they split in to three-fold degenerate (i.e. triplet state) t_{2g} (d_{xy}, d_{yz} and d_{zx}) and two- fold degenerate (i.e. doublet state) e_g (for instance, $d_{x^2-y^2}$ and $d_{3z^2-x^2}$) orbitals as seen in figure. The t_{2g} orbitals are

lower in energy than the e_g orbitals because the later are aligned with the P-oxygen levels leading to a larger coulomb repulsion than in other directions. Mn^{4+} has three electrons in the outer d-shell that can be considered as localized in the three t_{2g} levels giving a total spin $S=3/2$.
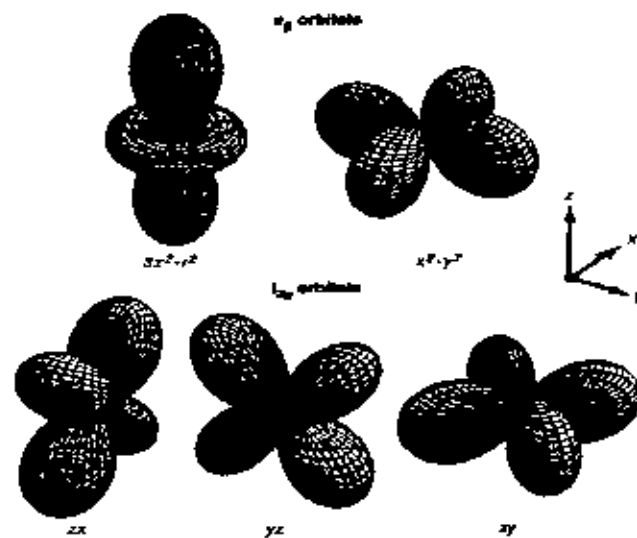
Figure : 2.4 The triplet t_{2g} orbital and doublet e_g orbital in Mn ion

The two e_g levels remain empty. On the other hand, Mn^{3+} has an extra electron that fills one of the e_g levels (S=2). This single electron is unstable. These e_g levels are the active one for conductivity. These levels hybridize with oxygen p-levels [43] constituting the conduction band whose bandwidth depends on the overlapping of the e_g orbitals of the Mn and the p-levels of the oxygen. The concentration of holes in the e_g based on x. For x <0.5, carries are holes while for x>0.5, the carries are electrons with concentration 1-x, as determined by Hall measurements and thermoelectric

power. There is an antiferromagnetic superexchange coupling among t_{2g} levels of nearest neighbour ions. Superexchange is mediated by the non-magnetic ion (oxygen). Moreover, the hopping of the carriers from one Mn to another leads to an indirect ferromagnetic exchange interaction between the localized spins (Double exchange). Hence, if the carriers were localized, superexchange would dominate.

2.6 Phase Diagram of Doped Manganites

Mixed valance manganites are complex materials showing a rich variety of structural, magnetic and electronic phases. Phase transition may be induced by changing the composition, changing the temperature or sometimes by applying an external magnetic field. Usually structural, magnetic and electronic phase transition occurs simultaneously. Figure 2.5 shows the combined phase diagram of $La_{1-x}Ca_xMn_3O_{10}$ and $La_{1-x}Sr_xMn_3O_{10}$ [44]. With regard to magnetic and conducting properties the optimum composition of both Ca and Sr-doped Lanthanum manganite is given by x=0.33. The investigation regarded phenomena, which are usually expected to show a maximum close to the ferromagnetic transition, namely magneto caloric effect and colossal magnetoresistance. The phase diagram of $La_{1-x}Ca_xMn_3O_{10}$ shows that curie temperature of $La_{0.67}Ca_{0.33}MnO_3$ is about 260K. For $La_{0.67}Sr_{0.33}MnO_3$ T_c is about 370K. It was anticipated that by preparing solid solutions between these compounds it would be possible to tailor materials with a ferromagnetic transition temperature close to room temperature thus having optimum magnetic and electrical properties at ambient condition. At low temperature the resistivity is metallic, rising sharply while going through the ferromagnetic transition. The resistivity in the case of Sr doping remains metallic above the Curie temperature. The ferromagnetic transition in this compound is accompanied by a metal-insulator transition as evidence by the resistivity

rise and negative temperature co-efficient of the resistivity in most compounds above

T_c.
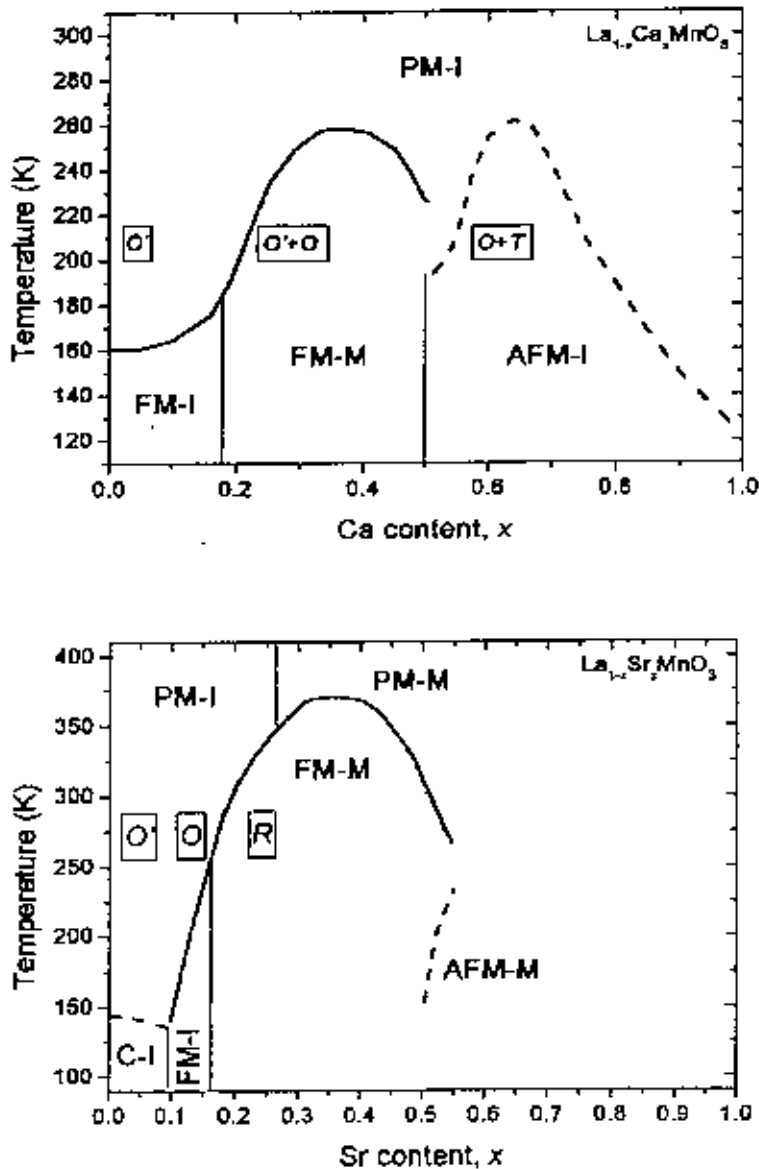
Figure: 2.5 Magnetic and electric phase diagram of $La_{1-x}Ca_xMnO_3$ (top plate) and $La_{1-x}Sr_xMnO_3$(bottom plate).Magnetic and electronic regions are indicated as follows: PM-I=paramagnetic insulator, PM-M=paramagnetic metal, FM-I=ferromagnetic insulator, FM-M=ferromagnetic metal, AFM-M= antiferromagnetic metal C-I=spin canted insulator. Symbols in boxes refer to structural phases(defined in text).Top plate adapted from Coey et. al (1999)[29], Schiffer et.al.(1995)[84].bottom plate adapted from Urushibara et.al.(1995)[38] and

2.7 Double Exchange Model

2.7.1 Theory of double exchange model

Manganese oxides when doped become ferromagnetic metals and exhibit remarkable magnetoresistive and metallic resistivity near the Curie temperature. This correlation was explained by Zener [45–46], proposed that ferromagnetism arises from indirect coupling among the manganese ion spins via the carriers, so called double exchange (DE) model. Zener has suggested a type of interaction between the spins of magnetic ions which he named "double exchange". This occurs indirectly by means of spin coupling to mobile electrons which travel from one ion to the next.

The physical properties of the doped perovskite manganite ($LaMnO_3$) involve a complex interplay between the spin, charge and orbital degree of freedoms, which strongly depends on the site of occupancy of the d-orbitals. The basic building of the manganites is the MnO_6 octahedra. In the cubic environment of the MnO_6 octahedron, hybridization and electrostatic interaction with oxygen 2p electrons will create a crystal field for the outer 3d electrons in Mn^{3+}. As the d-orbitals are five fold degenerate, so this crystal field affects the 5-fold degeneracy of d-electrons present in free Mn^{3+} ions by splitting the energy levels and forming lower-lying triply degenerate t_{2g} states and a higher doublet of e_g states [47,48]. The energy difference due to crystal field splitting (CFS) between t_{2g} and e_g levels for $LaMnO_3$ is approximately 1.5 eV. Due to strong intra-atomic hund's coupling, all electrons of Mn^{3+} and Mn^{4+} are aligned parallel in the ground state, leading to a total spin of S=2 and S=3/2 respectively. All three outer electrons of Mn^{4+} occupy the t_{2g} sites, while the extra electron of Mn^{3+} is situated in one of the e_g level. The t_{2g} orbitals overlap relatively little with the P-orbitals of nearby oxygen atoms. So that the t_{2g} electrons can be considered as forming a localized core spin (S=3/2). The e_g orbitals on the

other hand overlap with the p-orbital of neighboring oxygen atoms. Although strongly coupled ferromagnetically to the t_{2g} spin, the e_g electron ($s=1/2$) is more mobile and can hop between different Mn ions. Thus the partial degeneracy of the 3d orbitals has been removed by CFS.

The addition of divalent material in undoped $LaMnO_3$ changes the valence state of some Mn^{3+} to Mn^{4+} where there are three electrons in t_{2g} state and one electron in e_g state due to crystal field splitting. As $LaMnO_3$ is an antiferromagnetic insulator, the replacement of trivalent La^{3+} ions with any divalent cat ions (e.g. $Ca^{2+}, Sr^{2+}, Ba^{2+}$ etc.) will change some Mn ions to Mn^{4+} state without electrons. The vacant e_g state of Mn^{4+} makes it possible for e_g electrons in surrounding Mn^{3+} ions to hop into the e_g state Mn^{4+} as long as the localized t_{2g} spins of the neighbouring Mn^{3+} and Mn^{4+} ions are parallel. Zener interpreted feerromagnetism as arising from an indirect coupling between "Incomplete d-shell" of Mn^{3+} and Mn^{4+} via "Conducting electrons" of oxygen as shown in figure 2.6.
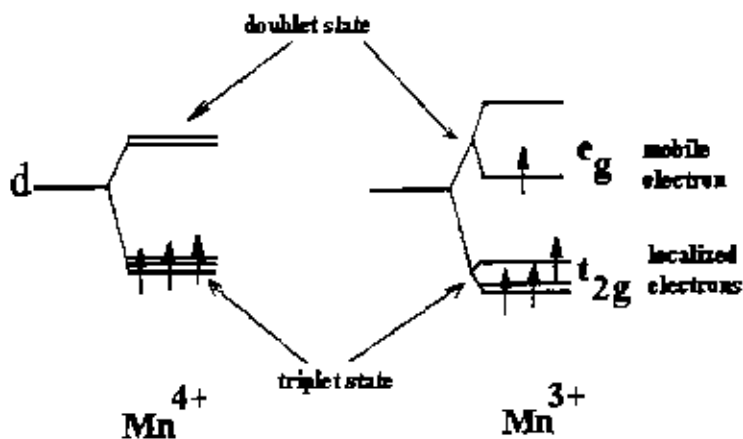
Figure: 2.6 Electron state of the outermost 3d energy level of the Mn^{3+} and Mn^{4+} ions.

In the parent compound $LaMnO_3$, the Mn ion is in 3+ state having electronic configuration $3d^4$ with three electrons occupy the t_{2g} levels and are coupled to a core

spin S=3/2 by the strong intra atomic hund's coupling and the fourth electron occupies one of the energetically degenerate e_g orbitals. Zener noted that on doping with a divalent ion on rare earth site, i.e. $RE_{1-x}AE_x MnO_3$ (where, RE=rare earth and AE=alkaline earth), the Mn ions become mixed valent with Mn fraction 'x' in the tetravalent Mn^{4+} ($3d^3$, $t_{2g}^3 e_g^0$, S=3/2) and '1-x' in the trivalent Mn^{3+} ($3d^4$, $t_{2g}^3 e_g^1$, S=2) state. He considered a cluster formed from oxygen and two Mn^{3+} ions. The basic idea of Double Exchange is that the configuration,

$$\varphi_1 = Mn^{3+}\text{-O-} Mn^{4+}$$
$$\text{and } \varphi_2 = Mn^{4+}\text{-O-} Mn^{3+}$$

are degenerate leading to a delocalization of the hole on the Mn^{4+} site or electron on the Mn^{3+} site.

$$t_{2g}^3 e_g^1\text{-O--}t_{2g}^3 e_g^0 \leftrightarrow t_{2g}^3 e_g^0\text{-O--}t_{2g}^3 e_g^1$$

$$t_{2g} \quad p_x \qquad t_{2g} \quad p_x$$

$$\text{Mn} \quad \text{O} \qquad \text{Mn} \quad \text{O}$$
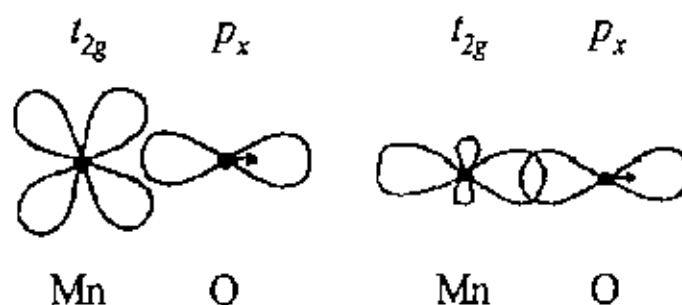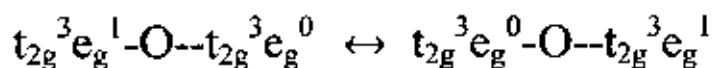
Figure: 2.7 Illustration of orbital overlaps between Mn t_{2g} and Mn e_g orbitals with a p orbital of a neighboring O ion.

The transfer of an electron occurs simultaneously from Mn^{3+} to O^{2-} and from O^{2-} to Mn^{4+}, this process is a real charge transfer process and involves overlap integral between Mn and O orbitals. Because of strong Hund's rule coupling J_H, the transfer matrix element has finite value only when the core spins of the Mn ions are aligned ferromagnetically. The Hund's rule coupling of degenerate states lifts the degeneracy and the system resonates between φ_1 and φ_2 if the core spins are parallel, leading to simultaneous occurrence of metallic conductivity and ferromagnetism. Zener made a estimation of electrical conductivity based on Einstein's relation and the diffusion constant of a hole located at a Mn^{4+} site which comes to be,

$$\sigma \approx \frac{xe^2}{ah}\left(\frac{T_c}{T}\right)$$

Where, σ = electrical conductivity, h = the Planck's constant, e = electronic charge, T_c =ferromagnetic transition temperature, x = concentration of Mn^{4+} ions and a = lattice parameter of Mn-Mn distance[49]. Zener's Model was based on the assumption that the manganites are uniform and homogenous without any form of coexisting clusters of competitive phases. In the double exchange model, Hund's coupling J_H is considered very large (in fact, $J_H \to \infty$), Hund's coupling forces the spin of the carriers to be parallel to the core spins. The minimization of the kinetic energy leads to ferromagnetic alignment of the core spins. Thus the necessary condition for this degeneracy (and hence, metallic conductivity) is that the spins of their respective d-shells point in the same direction because the carrier spin doesn't change in the hopping process and Hund's coupling punishes anti-alignment of unpaired electrons. The parallel coupling is of the order of magnitude of the hopping. Thus the double-exchange coupling leads to ferrmagnetism, and the effective transfer integral can be written

$$t = t_0 \cos(\theta/2)$$

The double-exchange model is based on the assumption that electron transfer takes place with spin memory, and the transfer integral t_0 depends on the angle between the adjacent core spins. An electron traveling from Mn^{4+} core with one spin direction to another Mn^{4+} come with a different spin direction causes a violation of Hund's first rule and energy is required to align the spins on the Mn site, where the electron arrives since the electron transfer is related to the angle between neighbouring magnetic moments, the double-exchange model explains why mixed valence manganites show a close relationship between transport properties and magnetism.

2.7.2 Importance of Double Exchange Model

The physical properties of the doped perovskite manganites ($LaMnO_3$) involve a complex interplay between the spin, charge and orbital degree of freedoms. Only Double-exchange mechanism can explain the behaviour of manganite perovskites. That's why it is very important. Double exchange and subsequent theories can explain the transport properties of manganites qualitatively.

In particular, magnetic properties are better described than electric properties (there is not a M-I transition for DE). But some manganites, a hole doped $La_{1-x}Sr_xMnO_3$, are metallic for the whole range of temperatures (figure 2.8). The fact is that lattice distortions complete with the bandwidth and a large bandwidth (as is the case of $La_{1-x}Sr_xMnO_3$) implies a more efficient double exchange interaction. In fact, Varma [50] and, more recently, Lyanda-Geller *et.al.* [51] have pointed out that Jahn-Teller phonons are not necessary to get the metal insulator transition and double exchange plus disorder, which leads to localization as proposed.
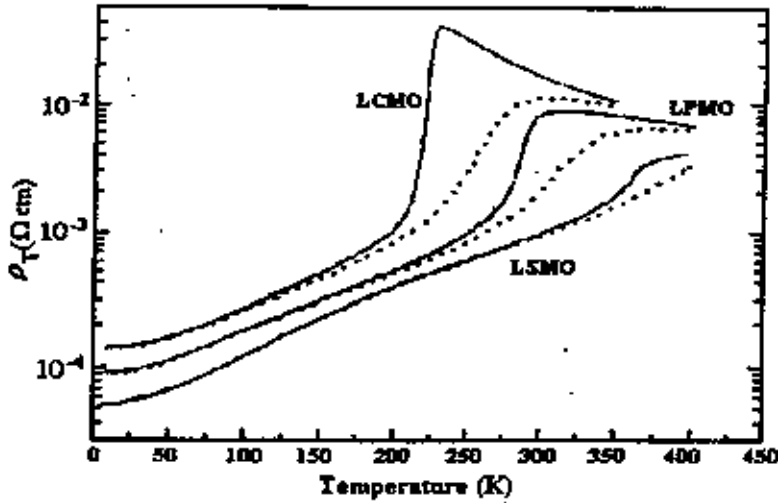
Figure 2.8: Temperature dependence of resistivity under zero magnetic field (solid lines) and other 7 T (dotted lines) for $La_{0.7}Ca_{0.3}MnO_3$, $La_{0.67}(Ca,Pb)_{0.33}MnO_3$ and $La_{0.77}Sr_{0.23}MnO_3$ [51].

2.8 Intrinsic and Extrinsic Magnetoresistance

The Physics of solids with strongly correlated electrons such as transition metal oxides (TMO) [52-54] and related compounds appears to be dominated by states that are microscopically and intrinsically inhomogeneous in certain range of temperatures and charge carrier densities. In magnetism, it is customary to distinguish an intrinsic property, which depends only on the bulk chemical composition and crystal structure, from extrinsic properties that are governed by the sample size and microstructure, for example, hysteresis is an extrinsic property, where as spontaneous magnetization is an intrinsic property. Intrinsic properties are best measured on single crystal and epitexial film. Magnetoresistance can be an intrinsic or extrinsic property. Intrinsic magnetoresistance is maximum close to the ferro-paramagnetic transition. The general form of the magnetization and the resistivity of CMR materials are shown in figure 2.9.

28

The aim of this section is to explain the difference between intrinsic and extrinsic magnetoresistance and to illustrate how they can be distinguished from experiment. Some results from the literature are used for exemplification.

When a magnetic field is applied, the peak on the resistivity moves toward higher temperature and dramatically decreases its height. The magnetic transition is accompanied by a change in the behavior of the resistivity with temperature. The system is metallic below the magnetic critical temperature T_c (namely, $d\rho/dt>0$) and insulator (activated) in the paramagnetic region ($d\rho/dt<0$). Approaching T_c from below the resistivity increases dramatically sometimes by order of magnitude [55].

For a single crystal there is negligible MR at low temperatures and with increasing temperature there is increasing negative MR. Correspondingly the magnetization show a rapid rise because of magnetic domain rotation at low applied field and a slow approach toward saturation at higher fields. The variation in the magnetization at various temperatures for the single crystal closely tracks the MR. Strongly suggesting that the suppression of magnetic fluctuations is the origin of negative MR, in the single crystal sample. Unlike the single crystal both polycrystalline samples (sintered at 1300°C and 1700° C) exhibit a sharp drop in the resistance at low fields followed by a slower background negative MR at higher fields. The sharp drop is greatest at the lowest temperatures and decreases with increasing temperature.

2.8.1 Intrinsic Magnetoresistance

Many research groups suggested that double exchange alone is not sufficient to explain the CMR. Besides this there are other mechanism-such as polaron formation due to the strong electron-phonon coupling or localized by spin fluctuations; this

supposed to drive the metal-insulator transition. The balance between the two competing mechanisms is very sensitive to an applied magnetic field that suppresses spin fluctuations and enhances the ferromagnetic order. But the essential transport mechanism[80] in the manganites has not yet been decided.
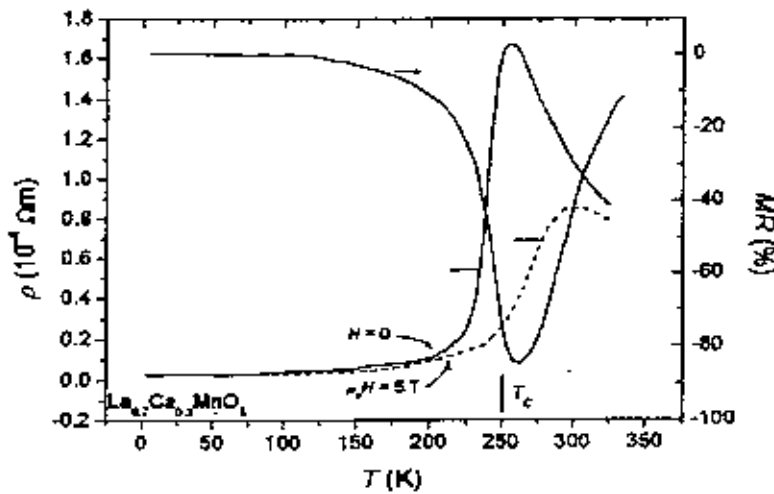
Figure 2.9 :Resistivity of single-crystalline thin film $La_{0.7}Ca_{0.3}MnO_3$ in zero magnetic field and in an applied field of 5T. The graph shows also the corresponding magnetoresistance. Adopted from Hundly et. al. [56].

Figure shows the temperature dependence of the zero field and $\mu_0H = 5T$ resistivities of a single-crystalline thin film $La_{0.7}Ca_{0.3}MnO_3$ sample (data obtained from Hundley et.al. [56]). The corresponding magnetoresistance, $MR=\rho_H/\rho_0-1$,is shown in the same graph. This sample has no internal grain boundaries so the magnetoresistive response is therefore entirely intrinsic.

The thin film substance shows a metal to insulator transition coinciding with the ferromagnetic to paramagnetic transition at the Curie temperature (250 K).

Qualitatively the temperature dependence of the magnetoresistance can be explained in terms of Zener's double-exchange mechanism. The simplest expression for conductivity is $\sigma = ne\mu$, where n is the number of carriers, and μ is there mobility. The metal-to-insulator transition could thus originate from either a change of the number of carriers or a change the mobility of the carriers. In the double-exchange theory the change of hopping mobility is the dominant effect on the conductivity. Below the ferromagnetic transition temperature the spin system is ferromagnetically ordered and the probability for electron transfer is high. The zero-field resistivity shows metallic-like temperature dependence with a positive slope. Around the curie temperature the spin system becomes disordered because the thermal energy exceeds the ferromagnetic exchange energy.

2.8.2 Extrinsic Magnetism

The polycrystalline sample exhibits a completely different behavior characterized by two features 1) Sharp increase of magnetoresistance at low fields followed by 2) linear background at higher fields. The slope of the high-field contribution is broadly temperature independent. The low field magnetoresistance, which is often termed LFMR(low field magnetoresistance), increases with decreasing temperature.

Following figure shows the comparism of the temperature dependence of magnetoresistance of a single crystalline manganite(an epitaxial thin film) with that of a polycrystalline thin film having the same composition($La_{0.67}Ca_{0.33}MnO_3$).Data was obtained from (Gupta et al.[57]).
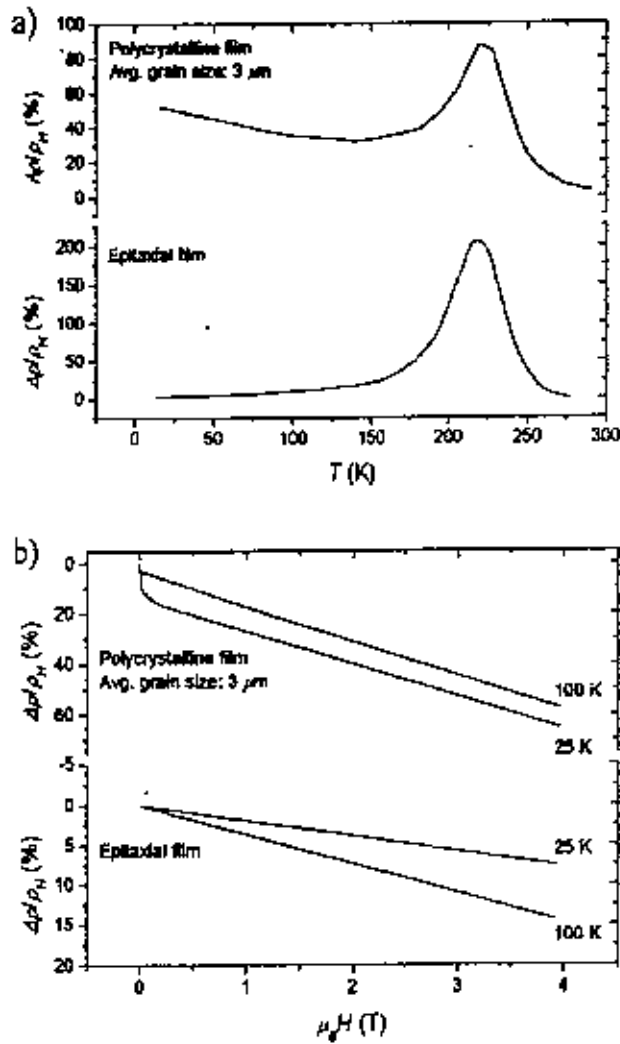
Fig2.10: Magnetoresistance temperature of poly-crystalline (top for a change of 0 to 2 T versus panel)and epitaxial (bottom panel) thin film $La_{0.67}.Ca_{0.33}MnO_3.b$) Magnetoresistance as a function of applied field taken at 25 and 100 K. Adopted from Gupta et al.[57].

Both samples show a magnetoresistance maximum near the Curie temperature, which can be ascribed to intrinsic magnetotransport (The CMR effect). For the epitaxial film the magnetoresistance vanishes at low temperatures, as expected for a single-crystalline material. However, the polycrystalline film shows an increasing magnetoresistance with decreasing temperature.

32

Figure 2.10 shows the dependence of magnetoresistance at two different temperatures below the ferromagnetic transition temperature. It has been suggested by Gupta et. al. [57] and Li et al.[58] that the low field magnetoresistance, which is observed in polycrystalline manganites, is due to spin dependent scattering grain boundaries. In ferromagnetic metals the exchange energy splits the conduction band into majority and minority carrier bands resulting in a spin imbalance at the Fermi level [59]. In mixed-valance manganites the majority and minority bands are separated by an energy gap arising from the strong intra-atomic coupling between the 3d e_g conduction electrons and the 3d t_{2g} core spins [60]. In the ferromagnetic state each grain in a polycrystalline manganite may constitute a single magnetic domain[57-59].

The polarized conduction electrons are easily transferred between Mn sites within a magnetic domain. However, an electron traveling across a grain boundary to an adjacent grain may become subject to a strong spin-dependent scattering leading to a high zero-field resistivity low external field can readily rotate the grain magnetization into parallel configuration and thereby cause a significant drop in resistivity and low field magnetoresistance. Spin-dependent scattering of polarized conduction carries is the dominant mechanism describing spin-valve effects in metallic GMR multilayers [61]. Hwang et.al. [60] offered a different explanation to the low field magnetoresistance effect observed below the Curie temperature. They compared the magnetoresistive properties of single-crystalline and polycrystalline $La_{0.67}Sr_{0.33}MnO_3$ and also observed LFMR (low field magnetoresistance)in the polycrystalline samples. They suggested that the effect was due to spin-dependent tunneling between adjacent grains separated by an insulating grain boundary consisting a tunnel barrier for the spin-polarized conduction electrons.

Spin dependent scattering or spin-dependent tunneling can explain the low-field magnetoresistance but fail to explain the linear high-field magnetoresistance. Evetts

et.al. [62] suggested that the high field magnetoresistance is associated with a magnetically mesoscopic disordered interface layer present in the vicinity of grain boundaries (figure-2.11) The transport mechanism in the interface layer is the same as in the bulk parts of the grains, but the layer has depressed Curie temperature and magnetization, which could be caused by strain, defects and weakened or absent bounds near the grain surface. The high-field MR could bo related to alignment of spins in the disordered inter-face layer.
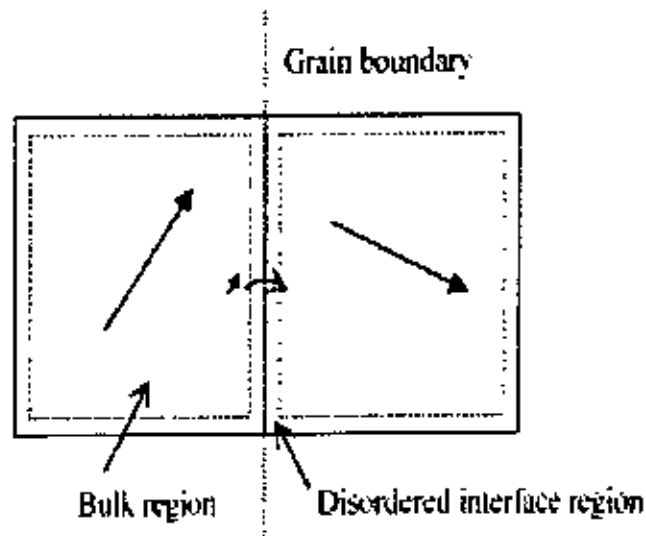
Figure: 2.11 Schematic illustration of grain-boundary transport in a polycrystalline mixed valance manganite. Each grain constitutes a single magnetic domain. The conduction electrons show a high degree of spin polarization inside the grains. When traveling across the grain boundary conduction electrons may be subject to a strong spin-dependent scattering, which can be reduced if a low external magnetic field aligns the magnetizations of the two grains. Spin alignment in the disordered surface layers gives raise to high-field magnetoresistance.

34

2.9 Transport properties of some polycrystalline materials

The grain boundary effect on resistivity and magnetoresistance of some polycrystalline manganites compounds were reported very early by Volger et. al.[63].The recent research was investigated by Hwang et al.[64] and Gupta et. al.[65].These authors compared the magnetoresistance and magnetization of $La_{0.67}Sr_{0.33}MnO_3$ single crystals and polycrystalline ceramics[64] and $La_{0.67}Ca_{0.33}MnO_3$ respectively. Both investigation found that the resistivity and magnetoresistance depend on microstructure [66].
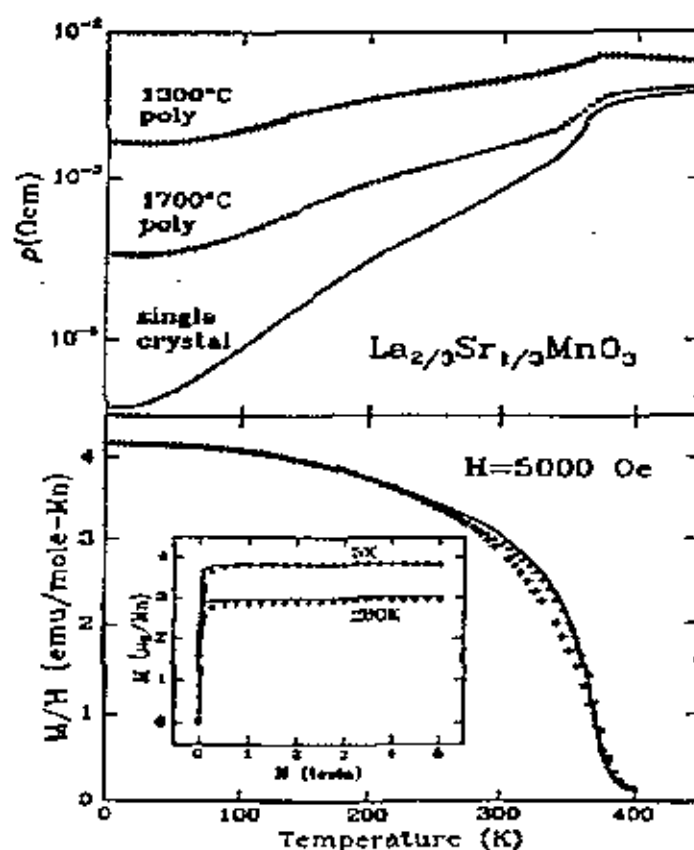
Figure: 2.12   Top panel: zero field resistivity of $La_{0.67}Sr_{0.33}MnO_3$ single crystal and polycrystals as a function of temperature. Bottom panel: magnetization of the sample as a function of temperature measured at B=0.5 T. The inset shows the field-dependent magnetization at 5 and 280K(reproduced from Hwang et. al.[64]).
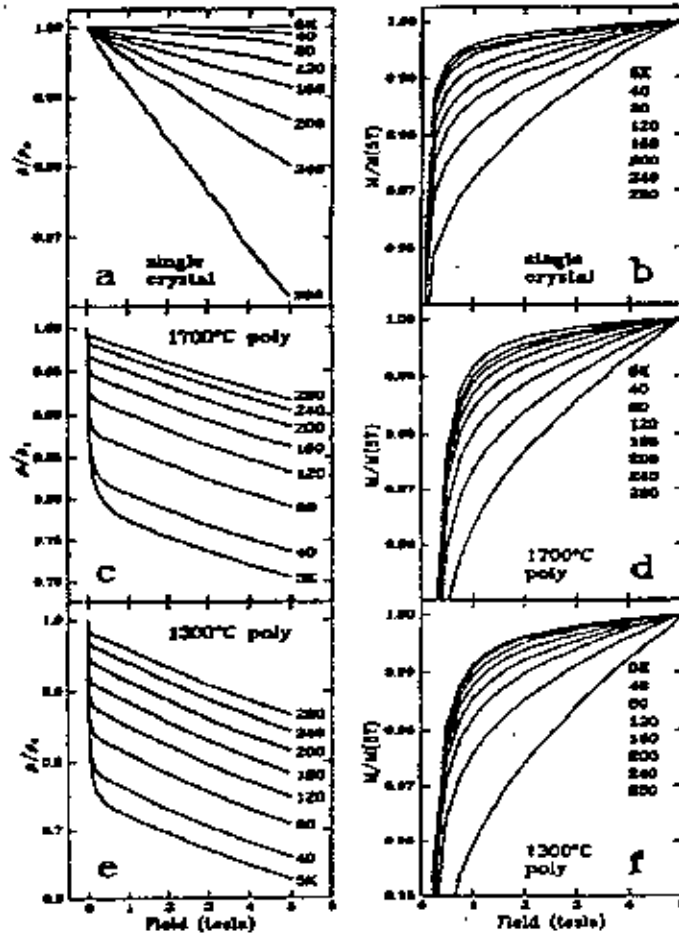
Figure 2.13 : Magnetoresistance data of the single crystal and polycrystalline samples :panels (a)(c) and(e)are the normalized resistivity ρ/ρo as a function of magnetic field. ρo denotes the zero-field resistivity. Panels (b)(d) and (f):magnetic field dependence of the normalized magnetization (reproduced from Hwang et. al.[64]).

Figure 2.12 shows the zero-field resistivity and the magnetization of the samples as a function of temperature. Where the low temperature resistivity depends strongly on the microstructure, the magnetization of three samples is virtually identical. The effect of the grain boundaries on the magnetoresistance is more dramatic. Figure 2.13 shows the investigation of some samples of field-dependent resistivity and magnetization. Where the single crystal shows a magnetoresistance is linear in magnetic field and

there is a sharp drop of resistivity in polycrystalline samples at low magnetic field and a linear dependence at higher magnetic field. The magnitude of the low-field magnetoresistance increases with decreasing temperature in contrast to the intrinsic magnetoresistance, that has a maximum near the Curie temperature and decreases with decreasing temperature. These results cannot be explained by the intrinsic magnetoresistance alone. Hwang *et.al.* [64] suggested that the low-field magnetoresistance in polycrystalline samples is due to spin polarized tunneling between misaligned grains.

2.10 Electron-Phonon Coupling and Jahn-Teller Distortion

The Double exchange and subsequent theories can only explain the transport properties of manganites qualitatively. However it overestimates the curie temperature of most manganites, can not describe the huge magnitude of the CMR effect, underestimates the resistivity values in the paramagnetic phase by several orders, and can't account for the existence of various antiferromagnetic phases, charge/orbital ordering, phase separation scenario and strong lattice effects/anomalies seen experimentally due to its inherent limitation for several manganites Millis *et. al.*(1995) [67] incorporated the idea that double exchange alone doesn't explain the resistivity of $La_{1-x}Sr_xMnO_3$. Their argument hinges mainly on an estimate of the curie temperature in a pure double exchange model which comes out to be an order of magnitude large. Millis *et.al.* calculated the resistivity within the double-exchange model including spin fluctuations and found that resistivity decreases below T_c and a positive magnetoresistance above T_c, both features in contradiction to the experimental results. Millis *et.al.*[72] argued that the electron-phonon coupling due to the dynamic Jahn-Teller distortion plays an important role, and that a strong interplay between electron-

phonon coupling, including charge localization, and Hund's coupling, generating a FM metallic phase, is responsible for the observed properties of manganites [68-71].

The strong e-ph coupling in manganites is mainly caused by the Jahn-Teller effect of Mn^{3+}. The JT effect causes local distortion of the crystal structure in which some of the Mn-O bonds become shorter and other longer. This breaks the local cubic symmetry, splits the degeneracy of the e_g levels on that site. By occupying the orbital with the lowest energy, the e_g electron can become effectively self-trapped to form together with the surrounding deformed lattice a quasi-particle called lattice polaron or Jahn-Teller polaron. This transport of lattice and spin distortions is also called as magnetic polaron. Calculation by Millis *et. al.* [68,15,72,73] predict the localization of charge carriers by temporal and spatial JT distortions around and above T_c. This would lead to the observed activated resistivity behavior in the paramagnetic base below T_c, the self-trapping of carriers ends leading to a relaxation of the lattice and an enhancement of the conductivity. In this theory both JT coupling and DE are needed to explain the properties in the various magnetic phases. This leads to the prediction of lower more correct T_c values, and can explain the high resistivity and large CMR effect in manganites. The close agreement between the theoretical predictions and the experimental evidence strongly indicates that the lattice effects in CMR materials are caused by the existence of small magnetic. Jahn-Teller polarons above T_c and melting of these entities below T_c. In this theoretical picture, the properties of manganites like the value of T_c, the magnitude of the CMR effect and whether the ground state becomes or stays insulating, depends on the relative strength of DE mechanism and the electron-phonon coupling, which is determined mainly by the nominal hole concentration x. There are various other theories/models e.g. Vibronic Model of Goodenough (1997) [74], Bi-polaronic Model of Alexandrov (1999) [19], Magnetoimpurity theory of Nagaev (2001) [20] etc. that explains some aspect or the

other of doped perovskite manganites, but satisfactory theory of manganese is still lacking.

Jahn-Teller distortion

The basic building block of the manganites are the MnO_6 octahedra[75].In the cubic environment of the MnO_6 octahedron, hybridization and electrostatic interaction with oxygen 2p electrons will create a crystal field for the outer 3d electrons in Mn^{3+} five-fold degeneracy state present in free Mn^{3+} ions due to crystal field forms lower lying triply degenerate states and higher doublet of e_g states. The low-lying t_{2g} triplet consists of the d_{xy}, d_{yz} and d_{zx} orbitals. The higher energy e_g doublet consists of the $d_{x^2-y^2}$ and $d_{3z^2-x^2}$ orbitals. Their lobes point in the direction of the O^{2-} ions, which raises their energy because of the stronger coulombic repulsion of the MnO_6 octahedra in doped $LaMnO_3$. The energy difference due to crystal field splitting (CFS) between t_{2g} and e_g levels for $LaMnO_3$ is approximately 1.5eV. Due to strong intra-atomic Hund's coupling, all electrons of Mn^{3+} and Mn^{4+} are aligned parallel in the ground state, leading to a total spin of S=2 and S=3/2 respectively. The t_{2g} orbitals overlap relatively little with the p-orbitals of nearby oxygen atoms, and forming a localized core spin S=3/2. The e_g orbital on the other hand overlap with the p-orbitals of neighbouring atoms. Although strongly coupled Ferro magnetically to the t_{2g} spin, the electron (S=1/2) is more mobile and can hop between different Mn ions. Thus the partial degeneracy of the 3d orbitals has been removed by CFS. The lattice motion usually breaks the remaining degeneracy.

This lifting of degeneracy due to the orbital lattice interaction is pronounced as Jahn-Teller co-operative effect. This effect tends to occur spontaneously because the energy

penalization of the lattice distortion grows as the square of that distortion, while the energy splitting of the otherwise degenerate orbitals is linear. This distortion can be estimated by the so-called Goldschimidt tolerance factor.

$$\Gamma = r_{Mn} + r_0 / \sqrt{2}(r_{A/B} + r_0)$$

$$\Gamma = \frac{r_{Mn} + r_0}{\sqrt{2}(r_{A/B} + r_0)}$$

Here r is the size of the different Mn, A, B and O ions in the system, $\Gamma=1$ for a cubic lattice and decreases as the difference in size between A and B increases. For oxides and fluorides the perovskite structure types are stable in the range $1.0 \geq \Gamma \geq 0.77$.

Tilting the octahedra can be measured with distottion of the Mn-O-Mn bond angle θ-$\theta=180°$ for cubic symmetry. For particular composition, θ can be the range from $150°$ to $180°$. This distortion affects the conduction band which appears as hybridization of the p-level of the oxygen and e_g levels of the Mn, which in turn depends on the geometric arrangement of the ions. The larger the overlap, the wider the band orbital overlapping decreases with the distortion and the relation between the bandwidth N and θ has been estimated as $N \propto \cos^2\theta$ [76].

Bandwidth is closely related to the magnitude of the critical temperature T_c that could be increased by chemical pressure. Two parameters are important here, the mean value of the cat ion sizes $<r_{A/B}>$ and its variance , $\sigma<r_{A/B}>^2 = <r^2_{A/B}> - <r_{A/B}>^2$. The main result is that a decrease of the cation disorder implies an increase of the critical temperature. In the ideal case $\sigma^2=0$ and a T_c as large as 520K could be achieved. Another cause of disorder is the larger size of Mn^{3+} (~0.72) with respect to Mn^{4+} (~0.5). This leads to a breathing distortion mode as shown in figure.
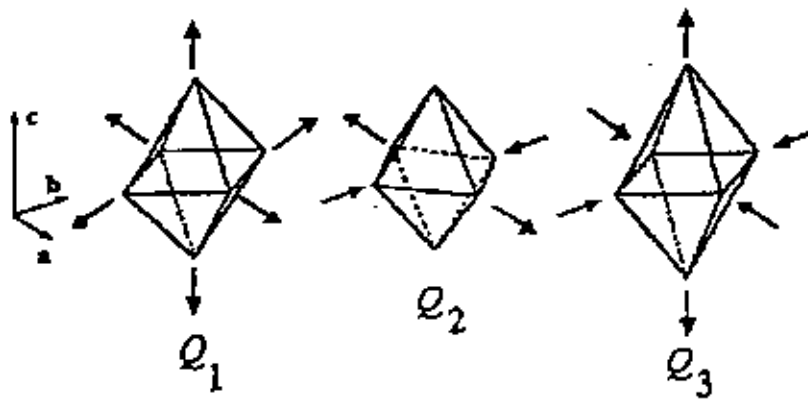
Figure: 2.14: Q_2 and Q_3 are the two Jahn-Teller modes of distortion of the oxygen octahedra associated to the splitting of the e_g levels of Mn^{3+}. these particular cases correspond to $Q_2>0$ and $Q_3>0$. Q_1 is the breathing distortion that occurs the different size of Mn^{4+} and Mn^{3+}.

For instance a Q_3 mode favours the occupancy of an orbital elongate on the Z-direction ($d_{3z^2-r^2}$). The interaction between the Jahn-Teller distortion modes and orbitals is called co-operative Jahn-Teller. When the carriers have certain mobility, the distortion of Mn^{3+} and Mn^{4+} ions are random and change with time. Therefore, electron-phonon coupling arises and in fact, Roder *et. al.* [77] claimed that it is necessary to take account of the lattice vibrations to explain the change in the curvature of the resistivity close to T_c. Moreover, due to large Hund's coupling, magnetic polar ions can also be formed [78].

It is well known that manganese perovskite present structural phase transitions for small values of x. The structure is rhombohedral at high temperature and orthorhombic with the lattice parameter ($\sqrt{2}a_0, \sqrt{2}a_0, \sqrt{2}a_0$) superstructure of the elementary cubic perovskite cell at low temperature. The critical temperature of this transition is ~700 K for x = 0 and decreases to 0 for x = 0.2. Asamitsu *et. al.* [79] Showed that this transition could be externally controlled by application of a magnetic field implying of a large spin-lattice coupling.

Definition: Jahn-Teller distortion

The Jhan-Teller effect causes local distortion of the crystal structure in which some of the Mn-O bonds become shorter and other longer [80,81]. This breaks the local cubic symmetry and splits the degeneracy of the e_g levels on that site. By occupying the orbital with the lowest energy, the e_g electron can become effectively self-trapped to form together with the surrounding deformed lattice a quasi particle called lattice polaron or Jahn-Teller polaron.

2.11 Types of magnetoresistance and their mechanism

A Classification of magnetoresistance phenomenon is based on the distinction familiar in magnetism between intrinsic properties such as anisotropy constants, which depend only on the crystal structure composition and purity, and extrinsic properties such as coercivity which depend on the structure on a mesoscopic or microscopic length scales.

Some classes of magnetoresistance are:

AMR - Anisotropy Magnetoresistance

GMR - Giant Magnetoresistance

PMR - Powder Magnetoresistance

BMR - Ballistic Magnetoresistance

CMR -Colossal Magnetoresistance

IMR - Intergrain Magnetoresistance

TMR - Tunneling Magnetoresistance

EMR - Extraordinary Magnetoresistance

VLMR - Very Large Magnetoresistance.

Some of their brief with the mechanism are given below:

2.11.1 Anisotropic magnetoresistance (AMR)

AMR effect is the change in resistance seen when the current flowing throw a sample changes from being parallel to the internal magnetization to being perpendicular to it resistance is high when current is parallel (or anti parallel) to the field and low when field and current are orthogonal. The dependence of the AMR effect is given by [82].

$$R_{tot} = R_{min} + \Delta R_{amr} \cos^2(\varphi)$$

Where,

R_{tot} = is the total electrical resistance

R_{min} = is the minimum electrical resistance

ΔR_{amr} = is the incremental AMR resistance

φ = is the angle between the current flow direction and magnetization direction in the material.

2.11.2 Giant magnetoresistance (GMR)

GMR is nothing but bearing the behavior of materials having alternating layers of ferromagnetic and nonmagnetic materials. GMR effect in the change in resistance in the magnetic multiplayer that occurs with a change in the relative directions of magnetization between layers. The GMR has also been observed in variety of inhomogeneous granular (cluster and alloys) system predominately comprised of Fe, Co, Ni and their various alloys in Cu, Ag and Au matrices. In granular magnetic systems, where small ferromagnetic grains (e.g. Fe, Co, Ni etc.) are embedded in an insulating matrix, the macroscopic properties depend on the metallic volume fraction 'x', the grain size and intergranular distance. When the relative orientation of grain is

43

antiparallel, it results in a minimum in conductance. When antiparallel grains are forced to be parallel by the application of a magnetic field, conductance increases and results in large magnetoresistance. On the other hand, in magnetic multilayers spin dependent scattering (SDS) at the interface is responsible for the GMR effect. The GMR relies on the fact that electron spin is conserved over a distances of up to several tens of nm, which is greater than the thickness of a typical multilayers, i.e. electric current in the trilayer flows in two channels, one corresponding to electrons with spin up projection and the other to electrons with spin down projection [83]. Since the ↑ and ↓ spin channels are independent (Spin is conserved) they can be regarded as two wires connected in parallel. Mott hypothesized that the electric current in FM metal is carried independently in two conduction channels that correspond predominately to the spin-up and spin-down s-p electrons. The spin up channel acts as a shunting current, lowering the resistivity of the complete stack of layers found considerable compared to when the moments are antiparallel. As a result the conduction electrons with spin parallel to the materials magnetization move freely, while the motion of those electrons with antiparallel orientation is implied via collusions with the atoms in the material. The dependence of The GMR effect is given by [84].

$$R_{tot} = R_{min} + \Delta R_{gmr} \sin(\varphi/2)$$

Where,

R_{tot} = is the total electrical resistance(tens of ohm)

R_{min}= is the minimum electrical resistance

ΔR_{gmr}= is the incremental GMR resistance

and φ= which varies between π and -π radius is the angle between the magnetization directions in the storage and sensing layers.

The GMR features are :

--Requires two materials

--Depends on relative orientation of two magnetization.

--magnetoresistance ratio of about 6%

--read-access times of below 50 ns were achieved for MRAM with GMR materials,

--low sense signal.

--magnetic cell would not work with sense lines narrower than about 1μm.

--there is a limit to how quickly the magnetization can change directions with distance.

2.12 Envisaged Applications of manganites

Perovskite manganites have a large potential for applications based on their various physical and chemical properties [85-87]. The magnetic field sensitivity of the transport properties, the strong metal insulator transition at the curie temperature, the electric field polarizibility of the material and its subsequent effect on the transport properties, the half metallicity of the electronic bands, etc. are properties of rare earth manganites that could be exploited in a variety of devices. Based on their properties, a number of devices are described below:

The magnetoresistance of manganites might be used in magnetic sensors, magnetoresistive read heads, and magnetoresistive random access memory. Magnetic sensors can be made from either thin films or single crystals and can be used to sense the magnitude of a magnetic field in one or several directions by choosing the right crystal form and de-magnetization factor. With a high density of grain boundaries and in tunnel spin valve structures a good low field magnetoresistive response will observed.

References

[1]   Jonker G.H. and Van Santen J.H., (1950), *"Ferromagnetic compounds of manganese with perovskite structure"*, Physica **16**, 337-349.

[2]   Van Santen J.H. and Jonker G.H., (1950), *"Electrical conductivity of ferromagnetic compounds of manganese with perovskite structure"*, Physica **16**, 599.

[3]   Jonker G.H. and Van Santen J.H., (1953), *"Magnetic compounds with perovskite structure III. Ferromagnetic compounds of cobalt "*, Physica **19**, 120.

[4]   Volger J., (1954), *"Further experimental investigations on some ferromagnetic oxidic compounds of manganese with perovskite structure"*, Physica 20-49.

[5]   Searle C.W. and Wang S.T., (1970), *"Studies of the ionic ferromagnet (La,Pb)MnO₃.v. Electric Transpport and ferromagnetic properties "*, can. J. Phys. **48**, 2023-2031.

[6]   Wang S.T. and Searle C.W., (1970), *"Studies of the ionic ferromagnet (La,Pb)MnO₃ . vi. Antiresonance and the ferromagnetic resonance line shape properties"*, Can. J. Phys. **49**, 387.

[7]   Jin S., Tiefel T.H., Cormack M.Mc., Fastnacht R.A., Ramesh R. and Chen J.H., (1994), *"Thousand fold change in resistivity in magnetoresistive La-Ca-Mn-O films"*, Science **264**, 413-415 .

[8]   Kusters R.M., Singleton D.A., Keen D.A., Megreevy R. and Hayes W., (1989), *"Polaron transport and lattice dynamics in colossal-magnetoresistance manganites"*, Physica **115**, B 362.

[9]   Von Helmholtz R., Wocker J., Holzapfel B., Schultz M. and Samwer K., (1993), *"Low field magnetotransport in manganites"*, Phys. Rev. Lett. **71**, 2331-2333.

[10]   Chahara K., (1993), *" Magnetoresistance in magnetic manganese oxide with intrinsic antiferromagnetic spin structure"*, Appl. Phys. Lett. **63**, 1990–1992.

[11]   Ju H. L., Kwon C., Li Q., Green R.L. and Venkatesan T., 1994 Appl. Phys. Lett. **65**, 2018.

[12]   Parkin S.S.P., (1995), *"Giant Magnetoresistance in magnetic nano structures"*, Annu Rev. Mett. science **25**, 357-388.

[13]   Sun J.R., Rao G.H. and Liang J.K., 1997 Appl. Phys. Lett. **70**, 1900 .

[14] Hwang H.Y., Cheong S.W., Radaelli P.G., Marezio M. and Barlogg B., 1995 Phys. Rev. Lett. **75**, 914.

[15] Millis A.J., (1998), *"Lattice effects in the magnetoresistive manganese perovskites"*, Nature **392**, 147.

[16] Roder H., Zang J. and Bishop A.R., (1996), *"Electronic excitations in $Bi_2Sr_2CaCu_2O_8$: Fermi surface, dispersion, and absence of bilayer splitting"*, Phys. Rev. Lett. **76**, 1536.

[17] Zang J., Bishop A.R. and Roder H., (1996), *"Double degeneracy and Jahn-Teller effects in colossal-magnetoresistance perovskites"*, Phys. Rev. B **53**, R 8840-R 8843.

[18] Goodenough J.B., (1997), *"Electronic structure of CMR manganites (invited)"*, J. Appl. Phys. **81**, 5330.

[19] Alexandrov A.S. and Bratkowsky A.M., (1999), *"Carrier Density Collapse and Colossal Magnetoresistance in Doped Manganites"*, Phys. Rev. Lett. **82**, 141-144.

[20] Nagev E.L., 1996 Usp Fiz Nauk **166**, 833.

[21] Ramakrishnan T.V., Krishnamurthy H.R., Hassan S.R. and Venketeswara pai., (2004), *"Theory of Insulator Metal Transition and Colossal Magnetoresistance in Doped Manganites"*, G Phys. Rev. Lett. **92**, 157203.

[22] Wollan E.O. and Koehler W.C.,(1955), *"Neutron diffraction study of the magnetic properties of the series of Perovskite-type compounds [(1-x) La, x Ca] MnO_3"*, Phys. Rev. **100**, 54.

[23] Dionne G.F., (1996), *"Magnetic exchange and charge transfer in mixed-valencec manganites and cuprates"*, Journal of Applied Physics, **79(8)**, 5172-5174.

[24] Millis J., (1998), *"Antiferromagnetic Short Range Order in a Two-Dimensional Manganite Exhibiting Giant Magnetoresistance"*, Phys. Rev. Lett. **80**, 4358 .

[25] Tokura Y., (1999), *"Colossal magnetoresistance oxides"*, Gordon & Breach Monographs in condensed Matter Science, London.

[26] Kusters R.M., Singleton J., Keen D.A., Greevy R.Mc. and Hayes W., (1998), *"Magnetoresistance measurements of the magnetic semiconductor $Nd_{0.5}Pd_{0.5} MnO_3$"*, Physica B **155**, 362.

[27] Tokura Y., Urushibara A., Moritomo Y., Arima T., Asamitsu A., Kido G. and Furukawa N., (1994), *"Giant magnetotransport phenomena in filling-controlled Kondo lattice system:$La_{1-x}Sr_xMnO_3$"*, J. Phys. Soc Jpn. **63**, 3931-3935.

[28] Von Helmot R., Wecker J., Holzapfel B., Schultz L. and Samwer K., (1993), *"Giant negative magnetoresistance in perovskite like $La_{2/3}Ba_{1/3}MnO_3$, ferromagnetic films"*, Phys. Rev. Lett. 71, 2331-2333.

[29] Coey J.M.D., Viret M. and Von Molner S., (1999), " *Mixed valence manganites,"* Adv. Phys. **48**, 167-293.

[30] Jin S., Mc Cormack M., Tiefel T.H. and Ramesh R., (1994), *"Colossal magnetoresistance in La-ca-Mn-O ferromagnetic thin films"*, Journal of Applied Physics, **76(10)**, 6929-6933.

[31] Alvysdas Lisauskas., (2000), *"Low frequency noise in thin film colossal magnetoresistors,"*, Ph D Thesis, department of condensed Matter Physics at the Royal Institute of Technology, Sweeden.

[32] Prellier W., Haghiri-Gosnet A.M., Mereey B., Lecoeur P.H., Hervieu M., Simon C.H. and Raveau B., 2000 Appl. Phys. Lett 77, 1023.

[33] Zhao Y.G, Rajeswari M., Srivastva R.C., Biswas A., Ogale S.B., Kang D.J., Prellier W., Chen Z., Green R.L. and Venkatesan T., (1999), *"Effct of oxygen content on the structural transport and magnetic properties of $La_{1-x}Mn_{1-\delta}O_3$ thin films"*, J. Appl. Phys. **86**, 6327- 6330.

[34] Goldschmidt V.M., (1926), Skrifer Norske Videnskops-Akad Osla,I Mat nat 8;Goldschmidt VM (1958), *"Geochemistry"*, Oxford University Press.

[35] Goodenough J.B., Kafalas J.A. and Longo J.M., (1972), *"Preperation method in solid State Chemistry"*, Hagenmuller(ed) Academic Press New York ;manthirum A. and Goodenough J.B.(1991) J. of Solid State Chemy.

[36] Goodenough J.B., (1996), *"Magnetism and the chemical Bond"*, Wiley-Interscience New York.

[37] Sun J.R., Rao G.H. and Liang J.K., (1997), *"Crystal structure and electronic transport property of perovskite manganese oxides with a fixed tolerance factor"*, Appl. Phys. Lett. 70, 1900.

[38] Urshibara A., Moritomo Y., Arima T., Asamitsu A., Kido G. and Tokura Y., (1995), *"Insulator – metal transition and giant magnetoresistance in $La_{1-x}Sr_xMnO_3$"*, Phys. Rev. B 51, 14103- 14109.

[39] Dho J., Kim W. and Hur N., (2001), *"Anomalous Thermal Hysteresis in Magnetization and Resistivity of $La_{1-x}Sr_xMnO_3$"*, Phys. Rev. Lett. **87(18)**, 187201-187205.

[40] Van Aken B.B., (2001), *"Structural response to electronic transitions in hexagonal and ortho-manganites"*, Ph D Thesis, Dutch foundation for fundamental Research on matter (MOF),University of Groningen, Netherlands.

[41] Huang Q., Santoro A., Lynn J.W., Rrwin R.W., Borchers J.W., Peng J.L. and Greene R.L., (1997), *"Structure and magnetic order in undoped Lanthanum manganite"*, Phys. Rev. B **55**, 14987- 14999.

[42] Goodenough J.B, (1970), *"Magnetism and the chemical bond"*, (Huntington:Krieger).

[43] Pickett W.E. and Singh D.J., (1996), *"Electronic structure and half-metallic transport in the $La_{1-x}Ca_xMnO_3$ system"*, Phys. Rev. B. **53**,1146-1160.

[44] Martin C., Maignan A., Hervieu M. and Raveau B., (1999), "Magnetic phase diagrams of $L_{1-x}A_xMnO_3$ manganites (L=Pr, Sm; A=Ca, Sr)", Phys. Rev. B **60**, 12191 – 12199.

[45] Zener C., (1951), *"Interaction between d shells in the transition metals"*, Phys. Rev. **81**, 440-444.

[46] Zener C., (1951), *"Interaction between the d-Shells in the Transition Metals. II. Ferromagnetic Compounds of Manganese with Perovskite Structure"*, Phys. Rev. **82**, 403 – 405.

[47] Anderson P. W., Hasegawa H., (1955) *"Considerations on Double Exchange"*. Phys. Rev. **100**, 675 – 681, University of Tokyo, Tokyo. Japan.

[48] Cox P.A., (1995), *"Transition Metal oxides: An Introduction to their Electronic Structure and properties"*, Clarendon press Oxford U.K.

[49] Röder H., Zang Jun. and Bishop A.R.,(1996), *"Lattice Effects in the Colossal-MagnetoresistanceManganites"*,Phys.Rev.Lett.76,1356–1359.

[50] Varma C.M., (1996), *"Electronic and magnetic states in the giant magneto-resistive compounds"*, Phys. Rev. B **54**, 7328-7333.

[51] Lyanda-Geller Y., Chun S.H., Salamon M.B., Golbart P.M., Han P.D., Tomioka Y., Asamitsu A. and Tokura Y., (2000),*"Charge Transport in manganites: hopping conduction, the anomalous hall effect and the universal scaling"*, condomat /0012462.

[52] Rao C.N.R. and Raveau B., (2 ed),(1998), *"Transition meatl oxides: Structure, Properties and synthesis of Ceramic Oxides"*, John Willey and Sons, Ine.

[53] Tokura Y. and nagaosa W., (2000), *"Orbital Physics in Transition-Metal Oxides"*, Science, **288**, 462-468 .

[54] Orenstein J. and Milis A.J., (2000), *"Advances in the physics of high-temperature superconductivity"*, Science **288**, 468-474.

[55] Maria Jose calderon Prieto, (2001), *"Colossal magnetoresistance of systems with magnetic and electric properties"*, Ph D Thesis, Instituto de Ciencia de Materials de Madrid (CSIC), Madrid.

[56] Hundley M.F., Hawley M., Heffner R.H., Jia Q.X., Neumeier J.J. and Teamer J.,(1995), *"Transport-magnetism correlations in the ferromagnetic oxide $La_{0.7}Ca_{0.3} MnO_3$"*, Appl. Phys. Lett. **67**(6), 860.

[57] Gupta A., Gong G.Q., Xiao G, Duncombe P.R., Lecoeur P., Trouilloud P., Wang Y.Y., Dravid V.P. and Sun J.Z, (1996), *"Grain boundary effects on the magnetoresistance properties of Perovskite manganite films"*, Phys. Rev. B, **54** (22), R 15629-15632.

[58] Li X. W., Gupta A., Xiao G and Gong G.Q., (1997),*"Low-field magnetoresistive properties of polycrystalline and epitexial perovskite manganite films"*, Appl. Phys. Lett. **71**(8), 1124.

[59] Gupta A., Sun J.Z.,(1999),*"Spin-polarized transport and magnetoresistance in magnetic oxides"*,Journal of magnetism and magnetic materials, **200**, 24.

[60] Hwang H.Y., Cheong S.W., Radaelli P.G, marezio M. and Batlogg B.,(1995), "Lattice *Effects on the Magnetoresistance in Doped $LaMnO_3$*", Phys. Rev. Lett. **75**(2), 914-917.

[61] Tumanski S., (2001), *"Thin film magnetoresistive Sensors"*, Bristol: Institute of Publishing.

[62] Evetts J.E., Blamire M.G, Mathur N.D., Isaac S.P., Teo B., Cohen L.F. and Macmanus-Driscol J.L., (1998), *"Defect-induced spin disorder and magnetoresistance in single-crystal and polycrystal rare-earth manganite thin film"*, Philosophical Transactions of the Royal Society, London A, **356**, 1593.

[63] Van den Born W.E. and Volger J.,(1998)., Phys. Lett. A **26**, 197.

[64] Hwang H.Y., Cheong S.W., Ong N.P. and Batlogg B., (1996), *"Spin polarized intergrain Tunneling in $La_{2/3}Sr_{1/3}MnO_3$"*, Phys. Rev. Lett. **77**, 2041-2044.

[65] Gupta A., Gong G.Q., Xiao G, Duncombe P.R., Lecoeur P., Trouilloud P., Wang W.W., Dravid V.P. and Sun J.Z., (1996), *"Grain boundary effects on the magnetoresistance properties of perovskite manganite films"*, Phys. Rev. B 54(22), R 155 629.

[66] Pi Li, Zhu Hong, Xu Xiao Jun and Zhang Yu Heng, (2001), *"Effect of the Substrate Orientation on the Transport Properties of La$_{0.67}$Sr$_{0.33}$MnO$_3$ Epitaxial Films"*, Chinese Phys. Lett. 18, 111-113.

[67] Millis A. J., Littlewood P. B. and Shraiman B.I.,(1995),*"Double Exchange Alone Does Not Explain the Resistivity of La$_{1-x}$Sr$_x$MnO$_3$"*, Phys. Rev. Lett. 74, 5144-5147.

[68] Millis A.J., (1996), *"Interplay between orbital, charge and magnetic orderings in R$_{1-x}$A$_x$MnO$_3$ (x=0, 0.5)"*, Phys. Rev. B 53, 8434-8435.

[69] Archibald W., Zhou J.S. and Goodenough J.B., (1996), *"Temperature dependence of electronic states in the t-J model"*, Phys. Rev. B 54, 14445-14454.

[70] Snyder G.J., Hiskes R., Di Carolis S., Beasley M.R. and Geballe T.H., (1996),*"Intrinsic electrical transport and magnetic properties of La$_{0.67}$Ca$_{0.33}$MnO$_3$ and La$_{0.67}$Sr$_{0.33}$MnO$_3$ MOCVD thin films and bulk material"*, Phys. Rev. B 53 14434-14444; Ziese M. and Srinitiwarawong C., (1998), *"Polaronic effects on the resistivity of manganite thin films"*, Phys. Rev. B 58, 11519-11525.

[71] Palstra T.I.M., Ramirez A.P., Cheong S.W., Zegarski B.R., Schiffer P. and Zaanen J., (1997)," *Transport mechanisms in doped LaMnO$_3$: Evidence for polaron formation"*, Phys. Rev. B 56, 5104-5107.

[72] Millis A.J., Shraiman B.I. and Mueller R., (1996), *"Dynamic Jahn-Teller Effect and Colossal Magnetoresistance in La$_{1-x}$Sr$_x$MnO$_3$"*, Phys. Rev. Lett. 77, 175-178.

[73] Millis A.J., Mueller R. and shraiman B.I. (1996), *"Fermi-liquid-to-polaron crossover. I. General results"*, Phys. Rev. B 54, 5389-5404.

[74] Goodenough J.B.. 1997 J. Appl. Phys. 81, 5330; 1999 Aust J. Phys. 52, 155; 1992 Ferroelectrics 130 77.

[75] Rodriguez-Martinez L.M. and Attfield J.P., (2001), *"Disorder-induced orbital ordering in La$_{0.7}$M$_{0.3}$MnO$_3$"*, Phys. Rev. B 63, 024424-024431.

51

[76] Garcia-Munoz J.L., Fonteuberta J., Suaaidi M. and Obradors X., (1996), "*Band-Width narrowing in bulk $La_{2/3}A_{1/3}MnO_3$ magnetoresistive oxides*", J. Phys.: Condens. Matt. **8**, L 787-L792.

[77] Roder H., Zang J. and Bishop A.R., (1996), "*Lattice effect in the colossal magnetoresistance manganites*", Phys. Rev. Lett. **76**, 1356-1359.

[78] Coey J.M.D.,Viret M., Ranno L. and Ounadjela K., (1995), "*Electron localization in mixed-valence manganites*", Phys. Rev. Lett. **75**, 3910-3913.

[79] Asamitsu A., Moritomo Y., Tomioka Y., Arima J. and Tokura Y., (1995), "*A structural phase transition induced by an external magnetic field*", nature **373**, 407.

[80] Ju S., Sun H. and Li Z., (2002), "*Study of magnetotransport in polycrystalline perovskite manganites*", Journal of Physics Condensed mater, **14**, L 631-L640.

[81] Toulemonde O., Millange F., Studer F., Raveau B., Park J-Hand., Chen C-T,(1999), "*Changes in the Jahn-Teller distortion at the metal-insulator transition in CMR manganites $(Pr,Nd)_{0.7}(Sr,Ca)_{0.3}MnO_3$*", J. Phys.: Condens. Matter **11**, 109-120.

[82] Ananth Hegdge and Ashwini Dwarkanath, "*Emerging memory technology*", CSE 597E, www. cse. psu. edu. typs.

[83] Chen S.H., Cheong S.W. and Hwang H.Y., (1997), "*Charge-ordered stripes in $La_{1-x}Ca_xMnO_3$ with $x > 0.5$*", J Appl. Phys. **81**, 4326.

[84] Kawano H., Kajimoto R., Kubota M. and Yoshizawa H. 1996 Phys. Rev. B **53**, 2202.

[85] Haghiri-Gosnet A.M. and Renard J.P., (2003), "*CMR manganites: physics, thin films and devices*", J. Phys D: Appl. Phys. **36**, R 127.

[86] Venkatesan T., Rajeswari M., Dong Z.W., Ogale S.B. And Ramesh R. 1999 Philos Trans Roy Soc A **356** 1661

[87] Venkatesan T., Rajeswari M., Dong Zi-Wen., Ogale S. B., Ramesh R., Stroud R., Blamire M., Palstra T. T. M. . Millis A. J., Maignan A., (1998), "*Manganite-Based Devices: Opportunities, Bottlenecks and Challenges [and Discussion]*", *Philosophical Transactions: Mathematical, Physical and EngineeringSciences*,Vol.356,No.1742

CHAPTER 3

SAMPLE PREPERATION AND EXPERIMENTAL TECHNIQUES

3.1 Introduction

The method of sample preparation, experimental techniques and characterization process are discussed in this chapter.

3.2 Material synthesis and sample preparation

The most commonly used method for the preparation of manganites samples are given below:

1.Solid-state reaction method

2.Solution method

3.Melt quenched or glass ceramic method

4.Thin film method

Solid-state reaction method

The present investigation is based on solid-state reaction method, in which occurs when the interacting materials have the gradients in chemical or electrochemical potential, temperature and surface free energy. In this reaction method atomic diffusion is very important. Such diffusion is very slow at normal temperatures because the entropy change is very small, for this all the solid-state reactions are exothermic in nature. The flow of atoms or ions or electrons from one equilibrium site to another is the phenomenon of diffusion in crystalline solids. In this reaction method, appropriate amounts of two or more chemical compounds are carefully ground

together and mixed thoroughly in a mortar or pestle or ball mills with acetone for homogenization. Ground powders are then calcined in air or in oxygen at a temperature above 1137K(900°C) for several hours to remove the unwanted oxides presents in the chemicals. Then they are reground and reheated. This process is continued until the mixture is converted in to the correct crystalline phase. Calcination is the heating process for the mixture of appropriate materials to convert into the correct crystalline phase. This heating process is done not less than 1173K(900°C).This calcined materials are then ground to fine powders and palletized in a hydraulic press. Sintering technique has been used to study the physical properties in the densified solid i.e. better densification solid is very important. After sintering the compact solid becomes more homogeneous and free from unreacted impurities. During sintering there is a great reduction in surface free energy arising from the reduction in total surface area. The sintering temperature is~1273K-1673K(1100°C) and sintering time is~5 hours.

3.3 Process for the preparation of present sample

The present polycrystalline bulk samples were prepared using the conventional solid-state reaction technique. High purity powder of La_2O_3 (99.9%), $SrCO_3$ (99.9%)and Mn_2O_3 (99.9%) were well mixed in a fixed amount and grounded in a ceramic mortar pestle for 3 to 4 hours in dry acetone media, then calcined at 1100°c in air in a heating furnace for 24 hours. The grinding and heating process were repeated for three times. After 72 hours of total calcinations, the powder was ground until it become finer. The calcined powder was pressed in to pellets of 12 mm diameter and 1-2 mm thick under a pressure of 12000 PSI for 1 to 2 minutes using a hydraulic press. The pellets was again placed in a boat and inserted into a furnace for sintering and oxidation at 1573K

(1100°C) in the furnace in air atmosphere. The temperature ramp was 10°C/min for both cooling and heating.

Methodology

The DC electrical resistivity for various polycrystalline samples was measured from room temperature down to liquid nitrogen temperature using standard four-probe method. The temperature dependence of resistivity, ρ(mΩ cm)at zero applied magnetic field for various polycrystalline samples and the corresponding behaviour in presence of 0.7 T applied magnetic field have been investigated in the temperature range 78K to 300K.

3.4 Characterization Technique

After the preparation of the samples, they need to be characterized in different ways to study their physical properties. It would provide the necessary feedback to improve the method of preparation of the grown materials. In the present investigation, powder X-ray diffraction was employed to characterize homogenization and other physical properties of the crystalline powder.

3.5 X-ray diffraction :Lattice planes and Bragg's law

X-rays are the electromagnetic radiation with typical photon energies in the range of 100eV-100KeV. For diffraction, only short wavelength X-ray(hard X-rays) in the range of a few angstroms to 0.1 Å(1KeV 120KeV) are used. Because the wavelength of X-rays is comparable to the size of atoms, they are ideally suited for probing structural arrangement of atoms and molecules in a wide range of materials. The

energetic X-rays can penetrate deep into the materials and provide information about the bulk structure.

X-rays primarily interact with electrons in atoms. When X-ray photons collide with electrons, some photons from the incident beam will be deflected way from the direction where they originally travel. Diffracted waves from different atoms can interfere with each other. If the atoms are arranged in a periodic fashion, as in crystals, the diffracted waves will consist of sharp interference maxima (peaks) with the same symmetry as in the distribution of atoms.
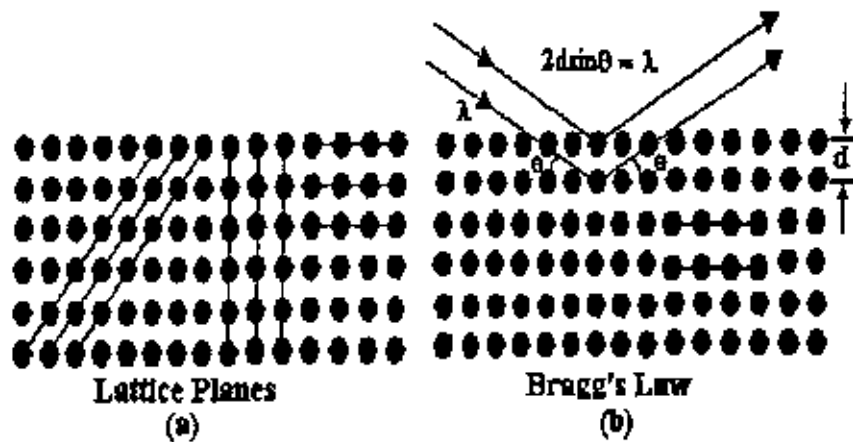
Figure 3.1: Bragg's law of diffraction (a) Different forms of lattice plans (b)Diffractions from atoms.

The peaks in an X-ray diffraction pattern are directly related to the atomic distances. Let us consider an incident X-ray beam interacting with the atoms arranged in a periodic manner, as shown in figure. The atoms, forming different sets of planes in the crystal. For a given set of lattice plane with an inter-planar distance of d, the condition for a diffraction (peak) to occur can be simply written as

$$2d_{hkl}Sin\theta = n\lambda$$

$$d_{hkl} = n\lambda/2Sin\theta$$

which is known as Bragg's law. In this equation, λ is the wavelength of the X-ray. θ is the scattering angle, and n is an integer representing the order of the diffraction peak. The Bragg's law is one of most important laws used for interpenetrating X-ray diffraction data.

3.6 Apparatus used for the present investigation

The apparatus which is commonly used for the present investigation are described as follows:

The liquid nitrogen cryostat

A liquid nitrogen cryostat was designed for the purpose magnetoresistive measurements. A schematic diagram of the liquid nitrogen cryostat is shown in figure. It is made up of nonmagnetic concentric stainless still tubes. It consists of two parts (an upper part and a lower part). Each part consists of three concentric tubes of the three different dimensions. The outer diameter of the upper part of the cryostat is 7.6 cm and inner diameter is 3.2 cm. The outer diameter of the lower part is 3.8 cm and inner diameter is 3.2 cm. It has three chambers; outer chamber is called vacuum chamber, the middle one is cryogen (liquid nitrogen) chamber and the inner most chamber is sample space. It is structured in such a way that the lower part of the cryostat can easily move between the pole pieces of the locally fabricated electromagneL
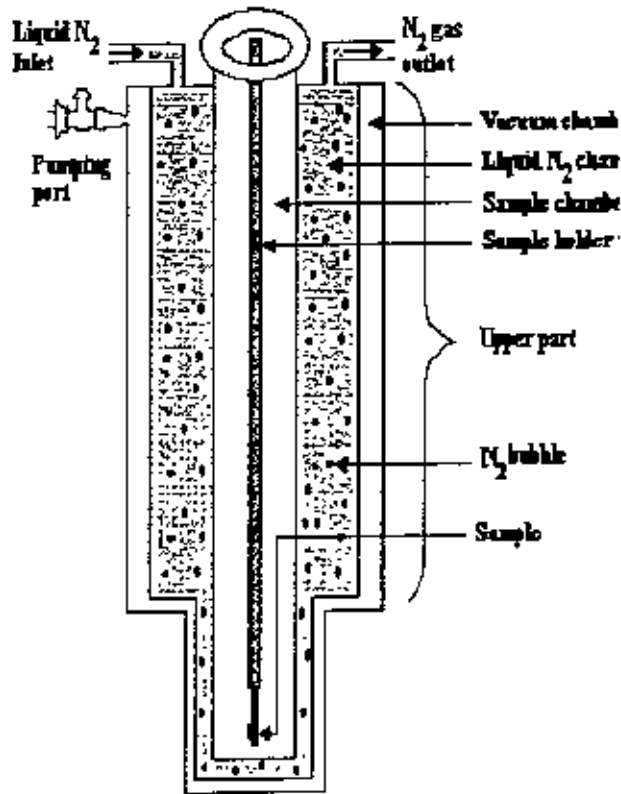
Figure : 3.2. Schematic diagram of the Liquid nitrogen cryostat.

Electromagnet

The electromagnet is used for magnetoresistance measurement as a function of temperature. (liquid nitrogen temperature to room temperature) and magnetic field. The schematic diagram of electromagnet used in the experiment is shown in figure 3.3. In the configuration of electromagnet, commercial milled still bar for the body and soft iron cylindrical rod for the pole pieces was used. The pole pieces were of 9.2 cm diameter and the pole gap varied from 0 to 10 cm. The current generated a dc magnetic field about 0.86 T in a pole gap of 3.8 cm.
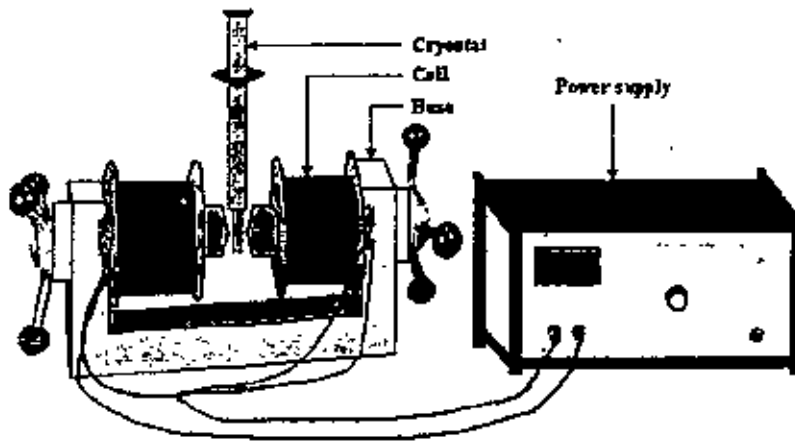
Figure: 3.3 schematic diagram of the electromagnet. Present investigation is shown in G 9.7.
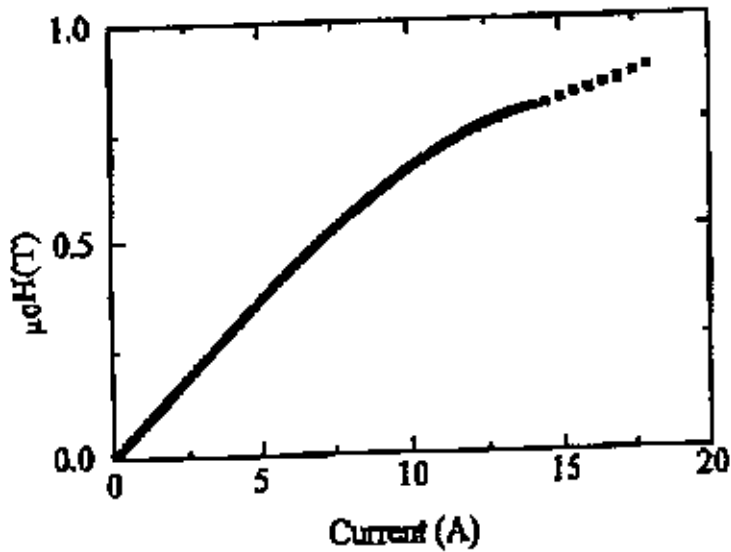
Figure: 3.4 shows the variation of magnetic field as a function of current with constant pole gap 3.8 cm.

Description of sample rod

This sample probe is used for four point resistance measurements. For the magnetoresistance measurements we applied magnetic field in the sample space. The schematic diagram of the sample rod used for the present experiments shown in figure 3.5 and also the calibration curve of the carbon glass resistor is shown in figure 3.6.
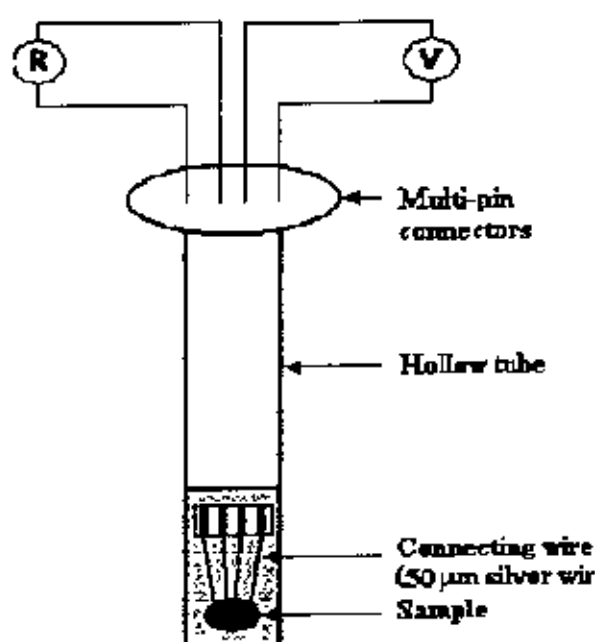
Figure :3.5 Schematic diagram of the sample holder.

The van der pauw method
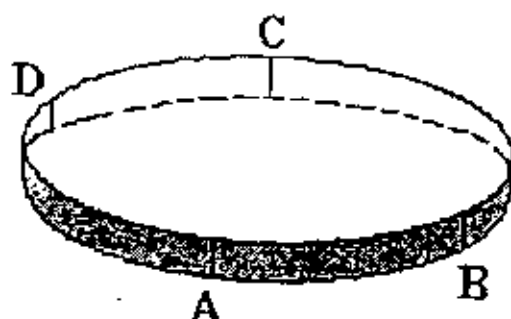
Figure :3. 6 The four electrical contacts on the circumstances of the disc shaped samples.

Figure 3.6 shows the physical representation of vander pauw techniques. It is based on four point measurements. There are four contacts on the circumference of the disc shape sample. For a fixed temperature, the resistance $R_{AB,CD}$ as the potential difference V_D-V_C between the contacts D and C per unit current I_{AB} through the contacts A and B. The current enters in the sample through the contact A and leaves it through B. The measurement will complete successfully if the certain conditions are fulfilled:

The contacts should be on the circumference of the sample.

The contacts should be sufficiently small

The sample is to be homogeneous and thin relative to the other dimensions.

The surface of the sample is to be singly connected, i.e. the sample doesn't have isolated holes.

Then,

$$R_{AB,CD} = \frac{V_D - V_c}{i_{AB}}$$ 3.1

Analogously we define,

$$R_{BC,DA} = \frac{V_D - V_c}{i_{BC}}$$ 3.2

The relation between $R_{AB,CD}$ and $R_{BC,DA}$ on which the Vander pauw method is based on,

$$\exp(-\frac{\pi d}{\rho}R_{AB,CD}) + \exp(-\frac{\pi d}{\rho}R_{BC,DA}) = 1$$ 3.3

Where,

d = the thickness of the uniform disc shaped sample

ρ = the resistivity of the materials

If d and the resistances $R_{AB,CD}$ and $R_{BC,DA}$ known,then in equation (3.4),ρ can be measured. In the general case, it is not possible to express ρ explicitly in known functions. The solutions can, however, be written in the form,

$$\rho(T) = \frac{\pi d}{\ln 2}\left(\frac{R_{AB,CD} + R_{BC,DA}}{2}\right) \; f\left(\frac{R_{AB,CD}}{R_{BC,DA}}\right)$$ (3.4)

Where f is a function only of the ratio $R_{AB,CD}$ only satisfy the relation

$$\cosh\left\{\frac{(R_{AB,CD}/R_{BC,DA})-1}{(R_{AB,CD}/R_{BC,DA})+1} \times \frac{\ln 2}{f}\right\} = \frac{1}{2}\exp\frac{\ln 2}{f}$$ (3.5)

Assuming $R_{AB,CD}/R_{BC,DA} = Q$ (3.5) becomes

$$\frac{Q-1}{Q+1} = \frac{\ln 2}{f}\; \text{arc cosh}\left\{\frac{\exp(\ln 2/f)}{2}\right\}$$ (3.6)

A plot of this function is shown in figure:
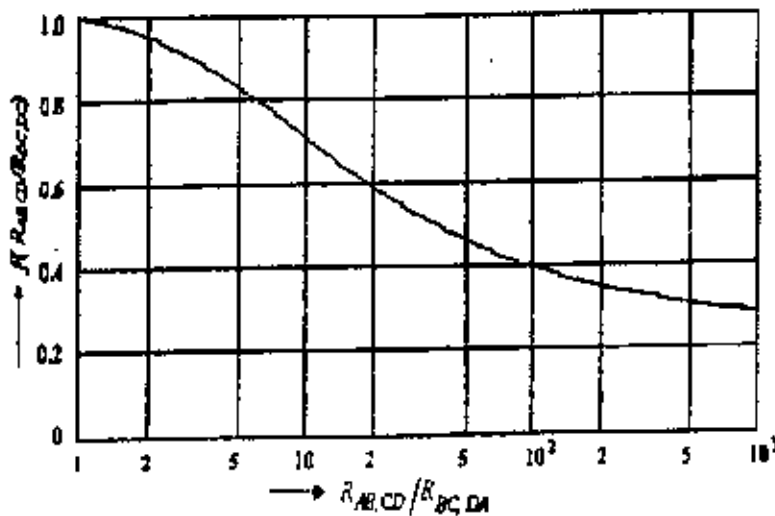
Figure: 3: 7 The function of f(Q) for determining the resistivity of the sample.

References

[1]   Scofield I.H., (1987),"*AC method for measuring low frequency resistance fluctuation spectra*", Review of scientific instrument, **58**, 985.

[2]   Van der Pauw L.I., (1958)," *A method of measuring specific resistivity < Hall effects and discs of arbitrary shape*", Philips Research Reports, **13**, 1-9.

[3]   Van der Pauw L.I., (1958),"*A method of measuring specific resistivity < Hall effects and discs of arbitrary shape*", Philips Technical Review, **20**, 220-224.

CHAPTER 4
RESULTS AND DISCUSSION

4.1 INTRODUCTION

In the present research work our approach was to study the (La, Sr) Ruddlesden-Popper series with doping by lanthanum La^{3+} of the Strontium Sr^{2-} i.e. electron doping so that the valence of the Mn would decrease from 4. Our present investigation is the layered compound for n=3 members and x=0.5, 1.0, 2.0, 2.5.

The results of DC electrical measurements including phase transitions, resistivity and magnetoresistance were measured from room temperature down to liquid nitrogen temperature both in zero field and in an applied magnetic field of 0.7T. Magnetoresistance (MR) measurements were carried out and the MR behavior was discussed as a function of magnetic field both at room temperature and at liquid nitrogen temperature. Activation energies for these polycrystalline samples were also calculated.

4.2 X-ray diffraction analysis

X-ray diffraction was carried out with an X-ray diffractometer using MoKα radiation (λ=0.71069Å). The diffraction study indicated that the crystal structure of the bulk samples were of single phases with orthorhombic perovskite structure having the lattice parameter a=22.68 Å, b=5.07 Å, c=5.85 Å.Table-4.1 gives the comparative peak position observed for polycrystalline samples $(La-D)_{n+1}Mn_nO_{3n+1}$ (n=3,D=Sr).The observed positions of the diffraction peaks are almost identical and thus confirmed the homogeneity of all the samples. Table 4.2 shows the interplanner distance d of each samples. which was measured by the Bragg's law of diffraction

$$n \lambda = 2d_{hkl} \sin\theta$$
$$d_{hkl}=(n\lambda)/ 2\sin\theta$$

X-ray diffraction pattern also indicates that the structure of the series polycrystalline samples has not noticeable change for various doped manganite systems.
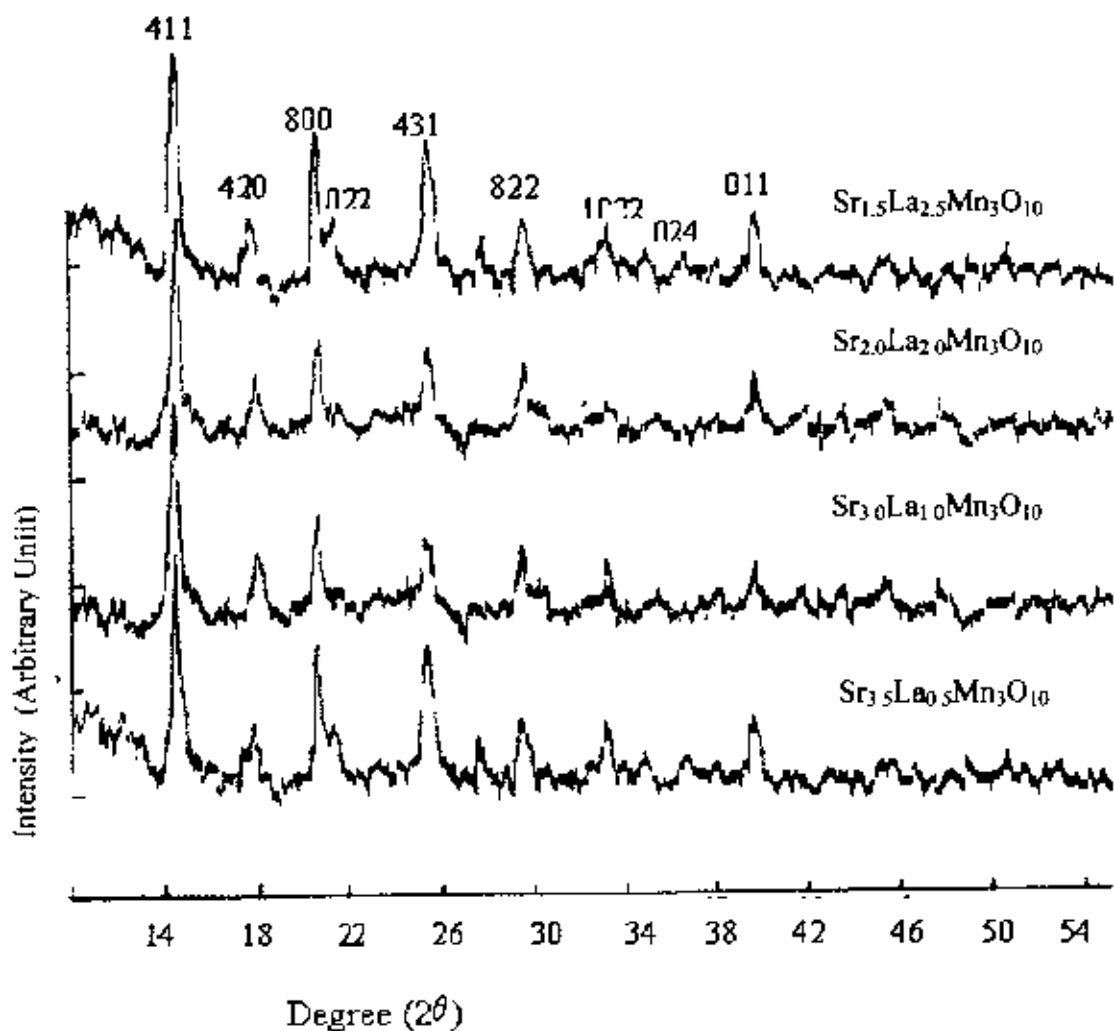

Figure 4.1 X-ray diffraction pattern for various polycrystalline samples

Table: 4.1 X-ray diffraction peak positions for various polycrystalline samples.

Samples	X-ray diffraction peak position 2θ(degree)							
	1st	2nd	3rd	4th	5th	6th	7th	8th
$Sr_{3.5}La_{0.5}Mn_3O_{10}$	14.40	17.20	20.56	25.60	29.56	33.20	36.20	39.60
$Sr_{3.0}La_{1.0}Mn_3O_{10}$	14.56	17.96	20.76	25.60	29.76	33.56	36.80	39.80
$Sr_{2.0}La_{2.0}Mn_3O_{10}$	14.52	17.96	20.76	25.40	29.56	33.20	36.48	39.68
$Sr_{1.5}La_{2.5}Mn_3O_{10}$	14.40	17.76	20.72	25.40	29.56	33.24	36.60	39.60

Table:4.2 Interplanner distance for various polycrystalline samples.

Samples	1st	2nd	3rd	4th	5th	6th	7th	8th
$Sr_{3.5}La_{0.5}Mn_3O_{10}$	2.83520	2.27654	1.97601	1.62139	1.47972	1.39108	1.24454	1.18498
$Sr_{3.0}La_{1.0}Mn_3O_{10}$	2.81189	2.27654	1.97221	1.61383	1.47919	1.39291	1.24200	1.17811
$Sr_{2.0}La_{2.0}Mn_3O_{10}$	2.81189	2.27654	1.97221	1.61383	1.47972	1.39291	1.24200	1.18498
$Sr_{1.5}La_{2.5}Mn_3O_{10}$	2.83520	2.30971	1.97597	1.61321	1.47919	1.39108	1.24200	1.18498

4.3 DC Electrical resistivity

Figure 4.2(a,b) and 4.3(a,b) shows the resistivity($m\Omega$ cm) behaviour as a function of temperature(K) for the samples $Sr_{3.5}La_{0.5}Mn_3O_{10}$, $Sr_{3.0}La_{1.0}Mn_3O_{10}$, $Sr_{2.0}La_{2.0}Mn_3O_{10}$ and $Sr_{1.5}La_{2.5}Mn_3O_{10}$ at 0T and 0.7 T respectively.

When the temperature is decreasing from room temperature the resistivity is increasing upto a certain point but below this temperature the resistivity of the samples is decreasing with decreasing temperature. This indicates that the behaviour of the material is changes from paramagnetic insulator to ferromagnetic metal [3,4] around a typical temperature, which is called the metal-insulator transition temperature.

The transition between ferromagnetic metallic and the paramagnetic insulating states in the manganites $S_{4-x}La_xMn_3O_{10}$ is characterized by a maximum in the electrical resistivity, which decreases in an applied magnetic field because of the suppression of spin fluctuations.

The metal-insulator (M-I) transition temperature of the samples is 133,139,147,175K, respectively in zero fields. The corresponding transition temperatures for these samples are found 139,150,156,188 K respectively in an applied magnetic field of 0.7T.
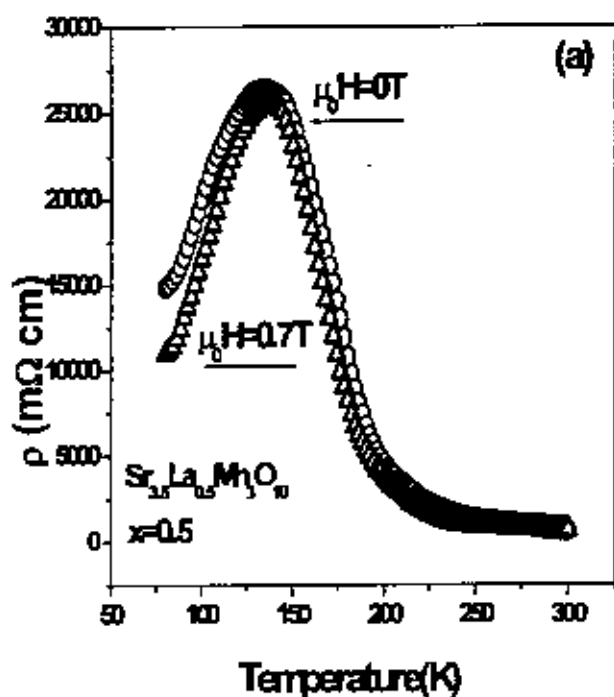
67
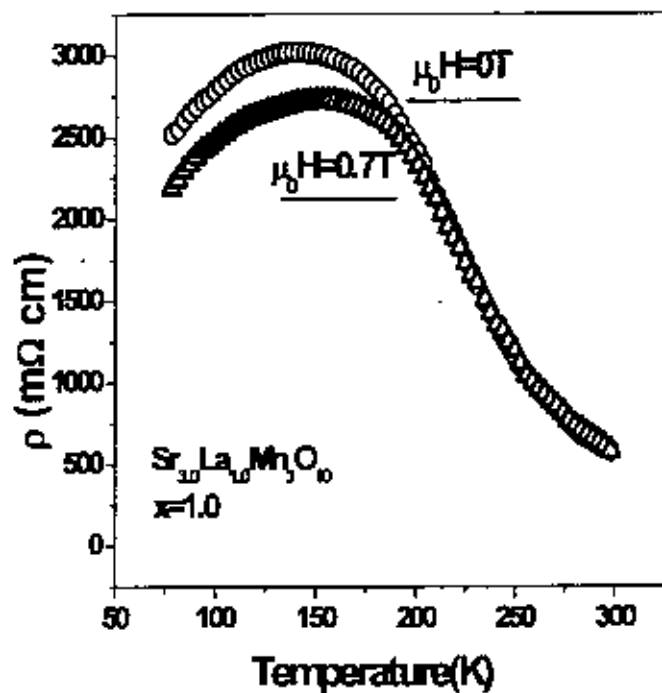
Figure 4.2:(a),Resistivity vs. temperature for sample $Sr_{3.5}La_{0.5}Mn_3O_{10}$, and (b)resistivity vs. temperature for sample $Sr_{3.0}La_{1.0}Mn_3O_{10}$, at 0 T and 0.7 T applied magnetic field.
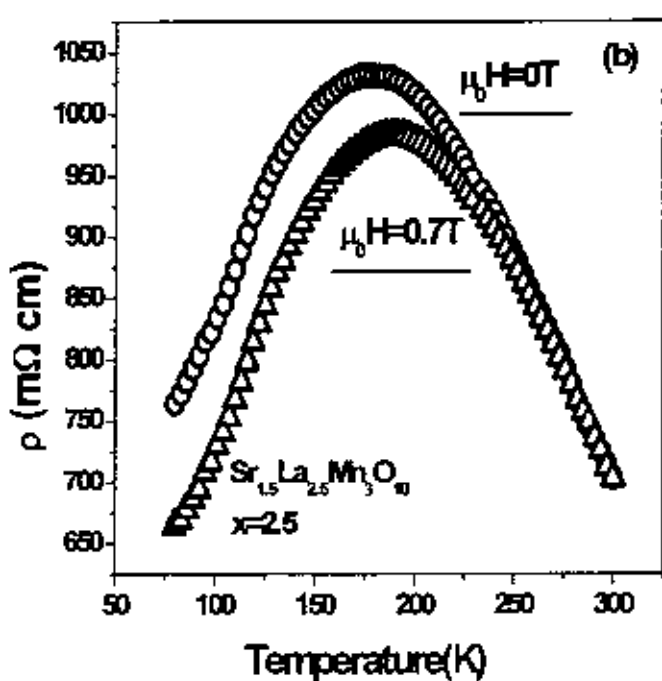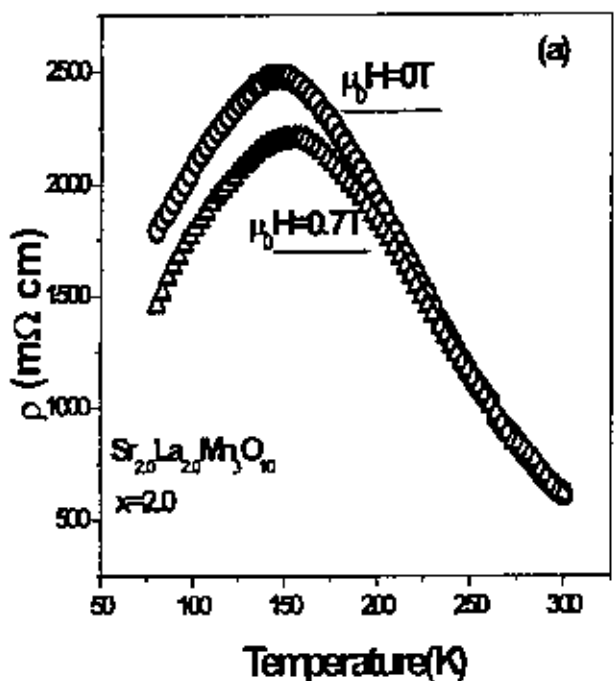

Figure 4.3:(a) Resistivity vs. temperature for sample $Sr_{2.0}La_{2.0}Mn_3O_{10}$ and (b)resistivity vs. temperature for sample $Sr_{1.5}La_{2.5}Mn_3O_{10}$ at 0 T and 0.7 T applied magnetic field.
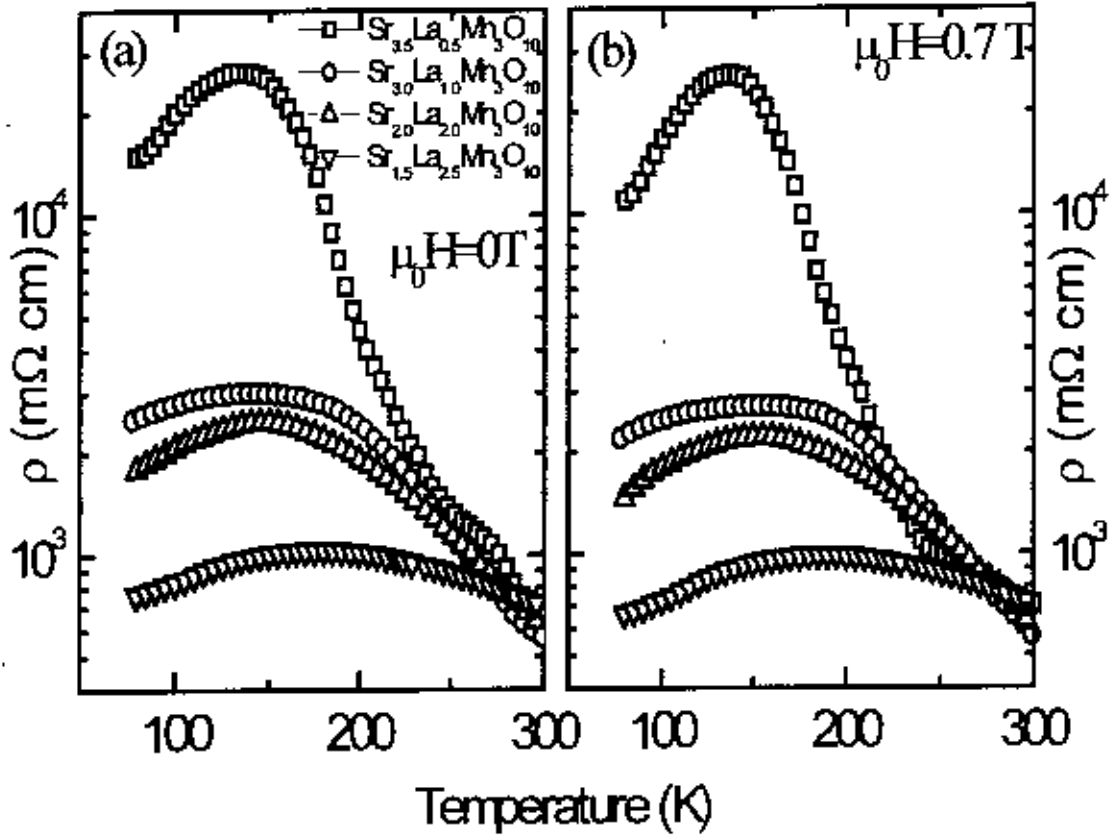
Figure 4.4: Comparative feature of resistivity vs. temperature curve for sample $Sr_{3.5}La_{0.5}Mn_3O_{10}$, $Sr_{3.0}La_{1.0}Mn_3O_{10}$, $Sr_{2.0}La_{2.0}Mn_3O_{10}$ and $Sr_{1.5}La_{2.5}Mn_3O_{10}$ at 0T and 0.7 T applied magnetic field.

This variation of M-I transition temperature can be explained in terms of the doping the divalent Sr with trivalent La of different values of x, which causes a conversion of Mn^{3+} to Mn^{4+}. It has been seen that Sr is non-magnetic and when Sr is replaced by La the transition temperature increases favoring metallic phase. Replacement of Sr with La, non-magnetic Sr is reduced and the concentration of La is increased. Reduction of non-magnetic Sr may enhance M-I transition temperature, the ferromagnetic to paramagnetic phase transition. For different values of x (0.5,1.0,2.0,2.5), where x is increasing the concentration of Sr is decreasing and the corresponding M-I transition

temperature is increasing. The M-I transition may be explained with the interaction mechanism between Mn ions.

In the case of undoped $SrMnO_3$ the ionic composition is $Sr^{3+}Mn^{4+}O_3^{2-}$. The electronic configuration of neutral Mn atom is $3d^5 4s^2$. If trivalent rare earth La atom is substituted by a divalent cation such as Sr, the following compound $Sr^{2+}Mn^{4+}O_3$ with the Mn valence 4+ will be obtained. Thus, the Mn ion in the $SrMnO_3$ compound will have 3-d electrons. The manganites $SrMnO_3$ is antiferromagnetic insulators. For a partial substitution, $La_{1-x}Sr_xMnO_3$ (0<x<1), the manganese ions become mixed valent, manganese fraction x in the tetravalent state Mn^{4+} $(3d^3)$ and (1-x) in the trivalent state Mn^{3+} $(3d^4)$, $La_{1-x}Sr_xMn_xMn_{1-x}O_3$ i.e. doping causes the conversion of a proportion number of Mn^{3+} to Mn^{4+}.

In the case of triple layered manganites $Sr_{4-x}La_xMn_3O_{10}$, when trivalent La ion is substituted in place of divalent Sr the charge neutrality is disturbed. To attain neutral charge configuration a part of Mn valency changes from 3+ to 4+ in the following manner and results the higher transition temperature.

$$Sr_{4-x}^{2+}La_x^{3+} Mn_x^{3+}Mn_{3-x}^{4+}O_{10}^{2-}$$
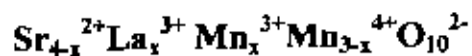
There is a mixed valent state of (x) and (3-x), x for trivalent and 3-x for tetravalent state. And a double exchange interaction [1] occurs within these states. When the doping level is increasing the concentration of Mn^{3+} is increasing and the proportion of non-magnetic Sr is decreasing. The conduction electron from Mn^{3+} state jump to oxygen p-orbital and from oxygen p-orbital to Mn^{4+} state. This metal-insulator (M-I) transition may be explained with the interaction mechanism between the manganese ions. Natures of the couplings are ferromagnetic when the interaction is in between

70

Mn^{3+} and Mn^{4+} ions, Ferromagnetic or antiferromagnetic behaviour arises for interaction between Mn^{3+} to Mn^{3+} and antiferromagnetic behaviour arises for interaction between Mn^{3+} to Mn^{4+}.

Thus doping the insulating material, in which Mn^{3+} exist, with the divalent ion Sr causes the conversion of a proportional number of Mn^{3+} to Mn^{4+}. Because of strong Hund's coupling, the electronic configurations are $Mn^{3+}(t_{2g}^{3}e_g^{1})$ and $Mn^{4+}(t_{2g}^{3}e_g^{0})$. The presence of Mn^{4+}, due to the doping enable the e_g electron of Mn^{3+} ion to hop to the neighboring Mn^{4+} ion via double exchange which mediates ferromagnetism and conduction.

In the present investigation the M-I transition temperature increase due to the external magnetic field, because of the suppression of spin fluctuations with the applied magnetic field in the paramagnetic region above T_p. The external magnetic field enhances spin order that ultimately decrease the resistivity and results higher transition temperature.

Table: 4.3 M-I transition temperatures T_p both at 0T and at 0.7 T applied magnetic field for various polycrystalline samples.

Samples	Transition temperature(K) Without field 0T	Transition temperature(K) With field 0.7T	Resistivity (mΩ cm) Without field 0T	Resistivity (mΩ cm) With field 0.7T
$Sr_{3.5}La_{0.5}Mn_3O_{10}$	134	139	26405.50	25460.04
$Sr_{3.0}La_{1.0}Mn_3O_{10}$	139	150	3017.74	2721.73
$Sr_{2.0}La_{2.0}Mn_3O_{10}$	147	156	2478.90	2203.86
$Sr_{1.5}La_{2.5}Mn_3O_{10}$	175	188	1031.73	983.71

In these polycrystalline samples there is a relation between the concentration of Mn^{3+} state and the transition temperature. From the previous investigation it has been seen that conduction electrons in Mn^{3+} state are responsible for interaction mechanism. Due to doping there is a mixed valence manganites of Mn^{3+} and Mn^{4+}. When the doping level increases the concentration of Mn^{3+} ion is increases. The hopping of e_g electrons from Mn^{3+} to Mn^{4+} is also increases which ultimately causes higher transition temperature and mediates the ferromagnetism. According to higher concentration of Mn^{3+} ion the transition temperature is increasing i.e. favouring the metallic behaviour.

4.4 Magnetoresistance as a function of applied magnetic field

The magnetoresistance MR is defined as,

$$MR\% = -\frac{\rho(H) - \rho(0)}{\rho(0)} \times 100$$

Where $\rho(H)$ and $\rho(0)$ are the resistivities in the presence and absence of magnetic field, respectively.
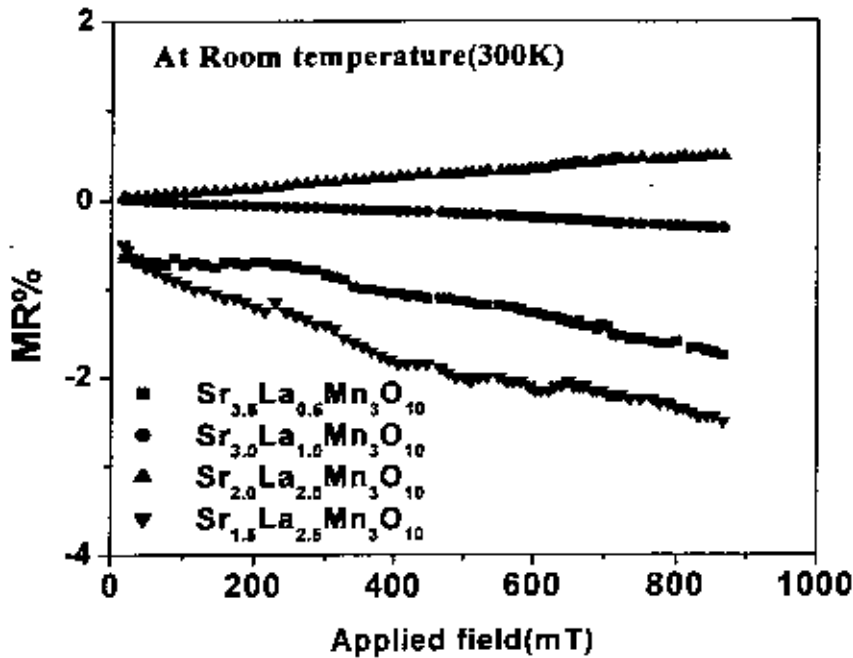
Figure 4.5: Magnetoresistance as a function of magnetic field at room temperature for various polycrystalline samples sintered at 1100°C for 5 hour
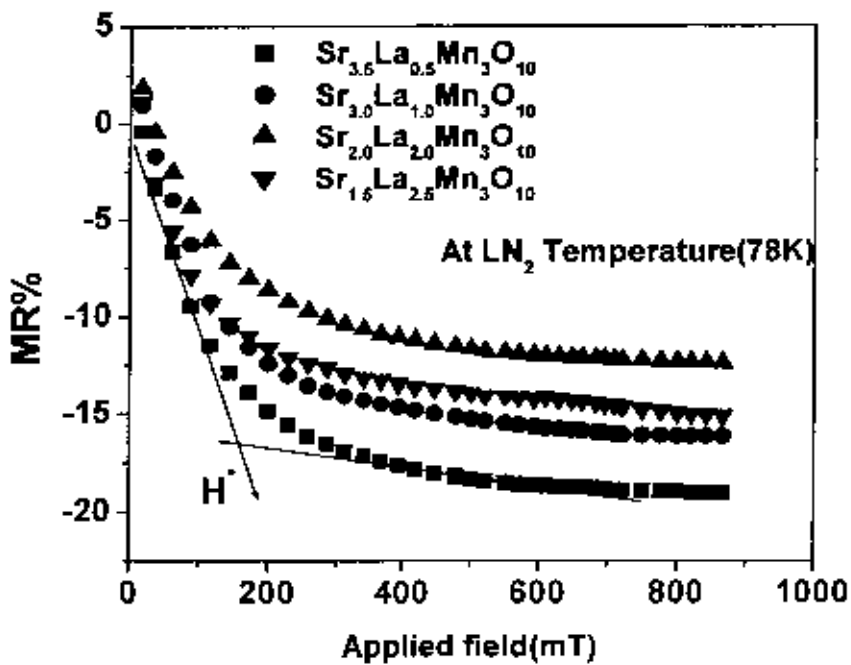

Figure 4.6: Magnetoresistance (MR) as a function of magnetic field at 78k for various polycrystalline samples sintered at 1100°C for 5 hour.

The MR as a function of magnetic field for all the samples was obtained at room temperature and at liquid nitrogen temperature. Room temperature MR is found to be very low almost 1.5%~2%, and is almost linear with field, which is shown in fig.4.5.At 78 K there is a sharp decrease in MR at low applied magnetic field. At low temperature (78 K) the field dependence of MR exists for an applied field of upto H^* as shown in figure 4.6. The magnetic field H^* designates the boundary of the two slopes. Beyond H^* the magnetoresistance is a weak function of the applied magnetic field. We observed about 10% ~ 17% MR at $H^* = 0.15T$~$0.20T$. About 13.00% of the MR is observed at $H^* = 172mT$ for $Sr_{1.5}La_{2.5}Mn_3O_{10}$. The total magnetoresistance for this sample is 19% under the application of 860-mT magnetic fields. As suggested by Pignard et.al. (1998) [2] such behaviour is associated with domain rotations caused by the applied field. This behaviour is due to the fact that the materials are subdivided into domains and low applied field is quite sufficient to align the domain spins and thus a sharp de crease in MR is observed. But to align the misaligned spins at the domain boundary region requires much larger field leading to weak field dependence

Table 4.4: H^* at 78 K for various polycrystalline materials.

Sample	Maximum H(mT)	H^*(mT)	MR%	Maximum MR%
$Sr_{3.5}La_{0.5}Mn_3O_{10}$		204	17.63	19.00
$Sr_{3.0}La_{1.0}Mn_3O_{10}$	860	156	14.00	16.12
$Sr_{2.0}La_{2.0}Mn_3O_{10}$		200	10.50	12.36
$Sr_{1.5}La_{2.5}Mn_3O_{10}$		172	13.00	15.10

The two slopes of MR at low temperature were explained by Hossain *et. al.* [5] in the following grain and grain boundary model. At $T<<T_c$, the material is in ferromagnetic domain or region. However, in the absence of field the magnetization of the grain of polycrystalline material will be like that of figure 4.7 (a). Also the individual spins at the grain boundary region are randomly oriented. In the absence of field, a carrier will suffer scattering from the unaligned magnetic domain, as well as disordered spin at the grain boundary region. By applying a low magnetic field, the magnetization of each grain starts to align towards the direction of the external magnetic field as shown in figure 4.7(b). For $H<H^*$, the MR changes rapidly with H but beyond H^*,MR was a weak function of applied magnetic field. This may be due to the reason that material is subdivided into domains, low field is quit sufficient to align the domains spins and thus a sharp decrease in MR is observed. However a large magnetic field is required to align the spins in domain boundaries as shown in figure 4.7(c) leading to weak field dependence.
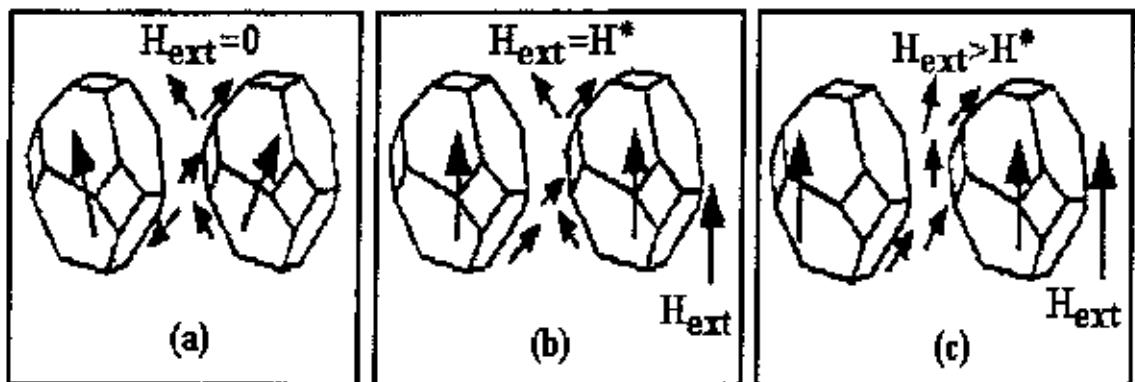
Figure 4.7 Explanation of the two slopes MR at low temperature (T<Tc)[5]

4.5 Magnetoresistance as a function of temperature

All the samples show magnetoresistance (MR) as a function of temperature. Figure 4.8 shows MR as a function of temperature for $Sr_{3.5}La_{0.5}\ Mn_3O_{10}$, $Sr_{3.0}La_{1.0}\ Mn_3O_{10}$, $Sr_{2.0}La_{2.0}\ Mn_3O_{10}$, $Sr_{1.5}La_{2.5}\ Mn_3O_{10}$ sintered at 1300°C for 1 hour. All the MR(T) curves were taken in presence of 0.7T applied magnetic field. Most of all shows low temperature MR, which increases linearly as the temperature decreases within the temperature range of 78K and 300K.
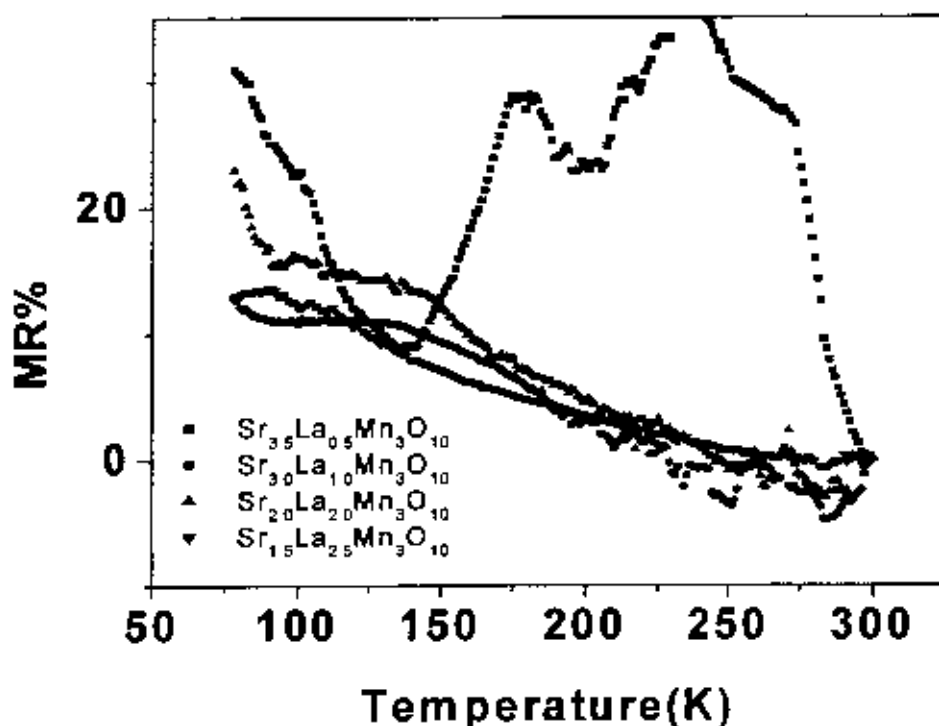
Figure 4.8:Magnetoresistance as a function of temperature at constant magnetic field 0.7T is shown for the samples $Sr_{3.5}La_{0.5}\ Mn_3O_{10}$, $Sr_{3.0}La_{1.0}\ Mn_3O_{10}$, $Sr_{2.0}La_{2.0}\ Mn_3O_{10}$ and $Sr_{1.5}La_{2.5}\ Mn_3O_{10}$.

4.5 Activation energy

The activation energy of a reaction is the amount of energy needed to start the reaction. It represents the minimum energy needed to form an activated complex during a collision between reactants. In slow reactions the fraction of molecules in the system moving fast enough to form an activated complex when a collision occurs is low so that most collisions do not produce a reaction. However, in a fast reaction the fraction is high so that most collisions produce a reaction.

The activation energy which explain the insulating –like behaviour of resistivity at temperature above T_p, can be calculate from the slopes of straight lines using the relation.

$$\rho = \rho_0 \exp (E_0/K_BT)$$

where, E_0 is the activation energy and K_B is the Boltzman constant. In figure 4.9 ln $\rho(T)/\rho(0)$ is plotted as a function of $1/T$ for various divalent alkaline doped sample at both without magnetic field and with magnetic field. The temperature region is considered from transition temperature to room temperature. The values of activation energies are shown in table 4.6.

The activation energy is then given by

$$E_0 = \ln[\rho(T)/\rho(0)]/1/T . K_B = slope \times K_B$$

Table: 4.5 Activation energy (m eV.) of the polycrystalline samples.

Samples	Applied magnetic field (0T)	Applied magnetic field (0.7T)
$Sr_{3.5}La_{0.5}Mn_3O_{10}$	58.37	45.32
$Sr_{3.0}La_{1.0}Mn_3O_{10}$	41.84	38.63
$Sr_{2.0}La_{2.0}Mn_3O_{10}$	38.81	35.31
$Sr_{1.5}La_{2.5}Mn_3O_{10}$	14.56	13.45

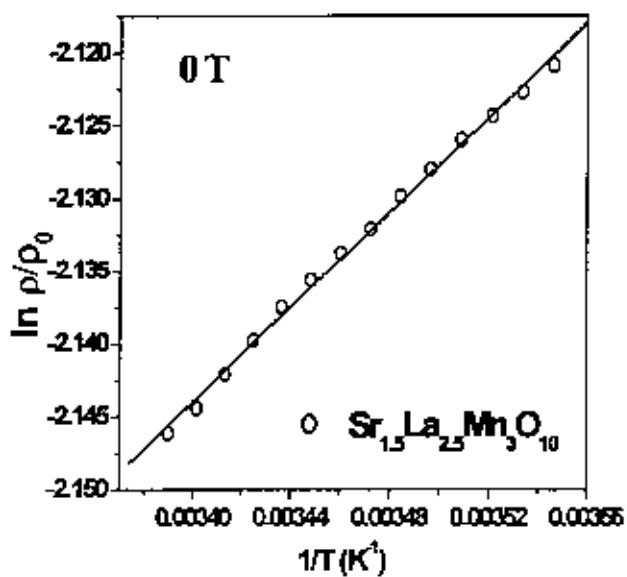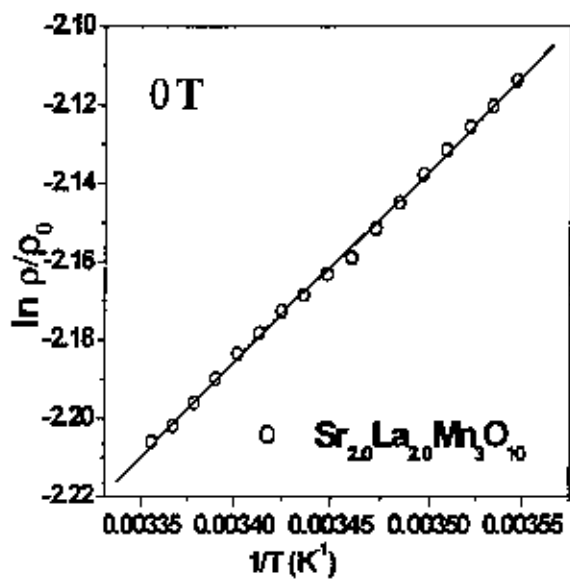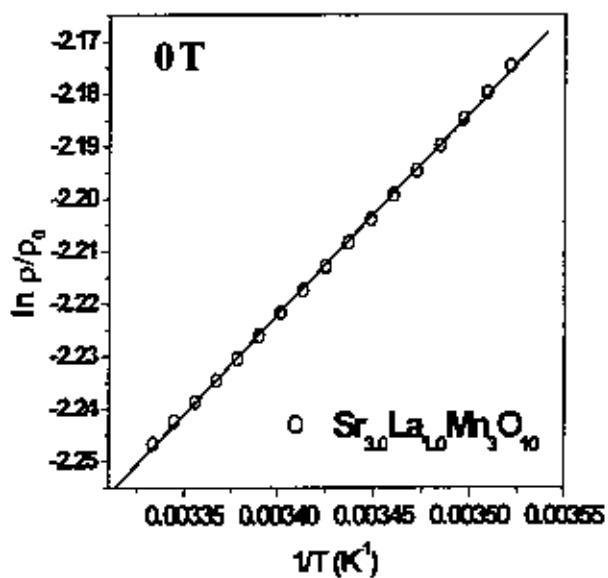All the samples show very good linear behaviour in the $\ln(\rho(T)/\rho(0))$ which suggest that conduction occurs through a thermally activated process.
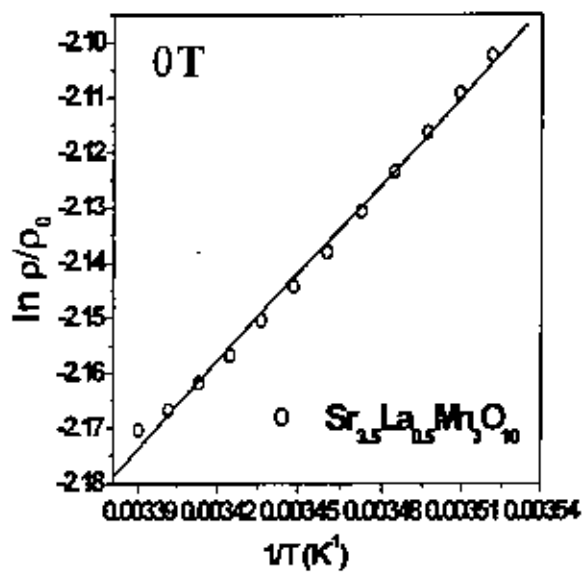
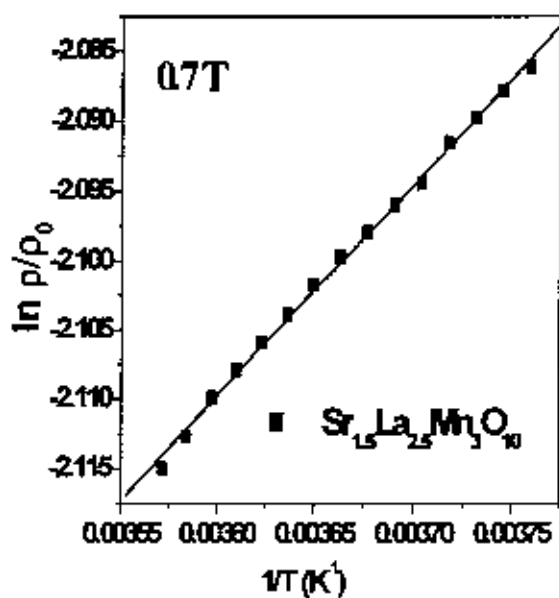Figure: 4.9 ln ρ/ρ(0) is plotted against $1/T(K^{-1})$ for various polycrystalline samples at 0T.
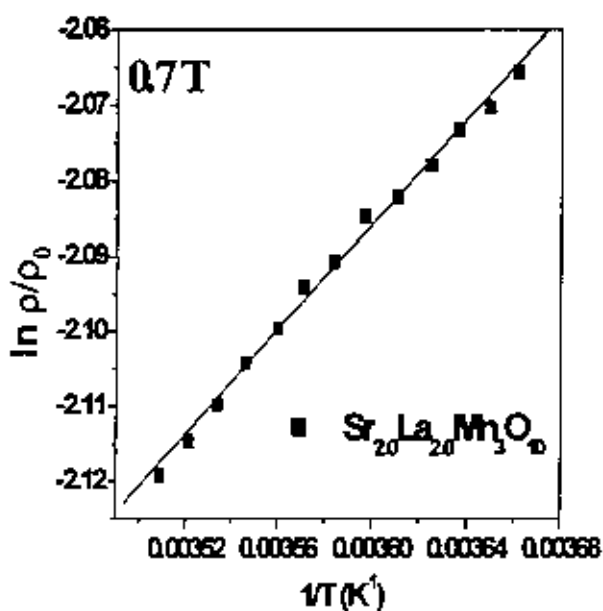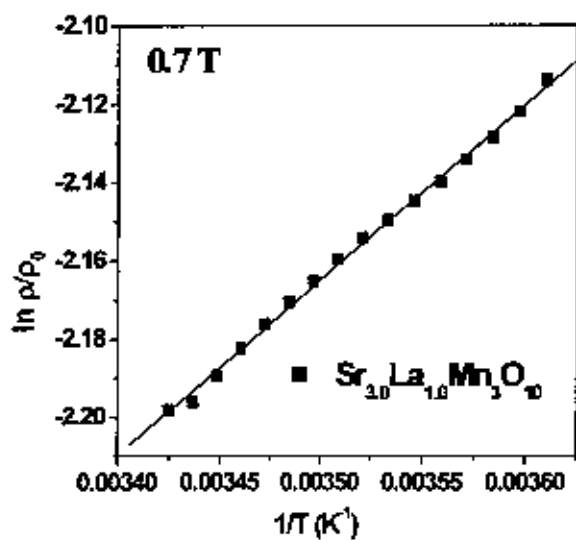
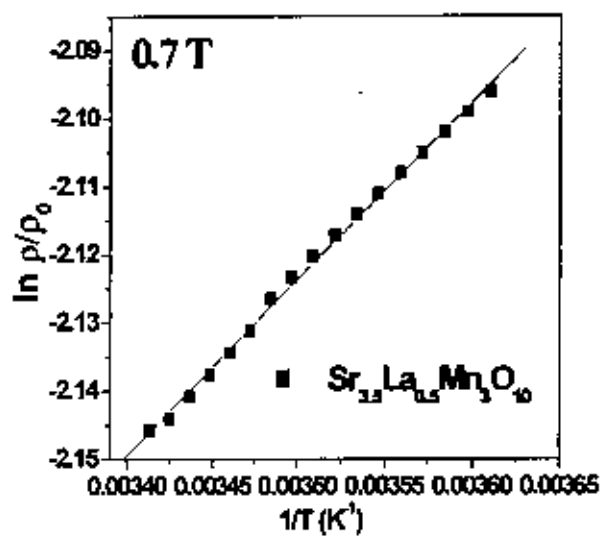Figure:4.10 : ln ρ/ρ(0) is plotted against 1/T(K⁻¹) for various polycrystalline samples at 0.7T.

[1]   Zener C., (1951),"*Interaction between d shells in the transition metals.ii.Ferromagnetic compounds of manganese with perovskite structure*",Phys. Rev. **82**,403

[2]   Pignard S.,Vincent H., Senateur J.P., Frohlich K and Souc(1998),"*Low field magnetotransport in manganites*", J. Appl. Phys lett.**73**, 999.

[3]   Witte N.S., Lincoln F.J, March R H., Kennedy S.J., (1997), "*Electrical and magnetic phases of the layered perovskite* $Ca_{1-x}La_xMn_3O_{10}$",Appl Phys Lett **72**(7).

[4]   Lago J., Battle P. D. and Rosseinsky M. J., (2000), "*Weak ferromagnetism and spin-glass behaviour of the n = 3 Ruddlesden-Popper compound* $Ca_4Mn_3O_{10}$: *a dc magnetization study*", J. Phys.: Condens. Matter **12**,2505-2524.

[5]   Hossain A.K.M.A., Cohen L.F., Damay F.,Berenov A.,MacManus-Driscoll J.L.,Alford N.M.,Mathur N.D.,Blamire M and Evetts J.E.,(1998), "*Influence of grain size on magnetoresistance properties of bulk* $La_{0.7}Ca_{0.3}Mn_{1-x}O_{3\pm\delta}$", J.Mag. & Mag.Mat.**192**, 263.

CHAPTER 5

CONCLUSIONS

In present research work, the magnetoresistive properties of the tripled layered perovskite manganites of $Sr_{4-x}La_xMn_3O_{10}$ were studied, where x=0.5,1.0,2.0,2.5. All the samples were sintered at temperature 1100°C for 5 hour. The DC electrical resistivity of all the samples were measured from room temperature (300K) down to liquid nitrogen temperature (78K), by using standard four probe van der Pauw technique for both 0T and 0.7T magnetic field respectively. Also the magnetoresistance measurement were carried out as a function of magnetic field H, keeping the temperature constant (both room temperature and liquid nitrogen temperature).

X-ray diffraction analyses show that the samples are homogeneous and single phase. It was observed that with the decrease in temperature, the resistivity of compounds $Sr_{3.5}La_{0.5}Mn_3O_{10}$, $Sr_{3.0}La_{1.0}Mn_3O_{10}$, $Sr_{2.0}La_{2.0}Mn_3O_{10}$ and $Sr_{1.5}La_{2.5}Mn_3O_{10}$, were increased reaching a maximum value at a certain temperature. With further decrease in temperature the resistivity get decreased. This temperature is the metal-insulator transition temperature and is generally very close to the curie-temperature T_c, the ferromagnetic to paramagnetic phase transition T_p. When divalent strontium is doped by trivalent lanthanum a mixed valence of manganites of Mn^{3+} and Mn^{4+} arises. With increasing doping concentration the content of Mn^{3+} increases and the corresponding transition temperature (T_p) is also increases. i.e. transition temperature is maximum for the doping concentration x=2.5.

All the samples undergo a transition from an insulating to a metallic behaviour as the temperature is decreased from room temperature and the transition temperature varies

82
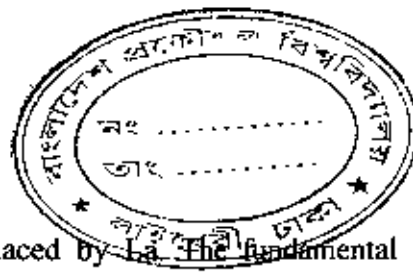
from 133K to 175K, when Sr was replaced by La. The fundamental mechanism leading to the appearance of transport behaviour like metal-insulator transition in the present investigated samples was explained within the framework of Zener double exchange mechanism.

It has been seen that Sr is non-magnetic and when Sr is replaced by La the transition temperature increases favouring metallic phase. Replacement of Sr with La, non-magnetic Sr is reduced and the concentration of La is increased. This ferromagnetic coupling enhances T_p, the ferromagnetic to paramagnetic phase transition.

The resistivity vs. temperature graphs with and without field show similar behaviour except the enhancement of M-I transition temperature by few Kelvin. This would be due to the suppression of spin fluctuations with the applied field in the paramagnetic region. The external magnetic field enhances spin order that ultimately decrease the resistivity and results higher transition temperature.

All the samples exhibits two distinct slopes in MR as a function of applied magnetic field. Highly sensitive low field MR was observed upto an applied magnetic field H^*. For $H < H^*$ the MR changes rapidly with H. Beyond H^*, MR has a weak dependence in applied magnetic field. This low field MR is expected due to polarization of electrons in magnetically disordered regions near the domain boundaries. However a large magnetic field is required to align the spins of the grain boundary region resulting in a weak dependence on H.

The plot of ln $\rho/\rho(0)$ vs. 1/T suggest that conduction occurred through a thermally activated process above the transition temperature.

83